

CHAPTER IV

RESULTS AND DISCUSSION

4.1 The Coir Fiber(Cocos nucifera Linn.)

Coir fiber is a unique fiber obtained from the fruit of coconut palm. The fibrous tissue lies between the tough exocarp and the hard shell (endocarp) which surrounds the kernel. Coir is a hard and tough fiber. Each fiber is polygonal to round in section. It is multicellular fiber with a central pore called lacuna (Figure 4.1). Each cell is round or polygonal in shape and $0.3-1.0 \times 10^{-3}$ m long with 12-14 μm diameter. The lumen size is estimated to be 5.7-7.5 μm . The chemical constituents of pure coir are cellulose (32-43%), lignin (40-50%), hemicellulose (0.15-0.25%) and pectin (2.75-4%)(1).

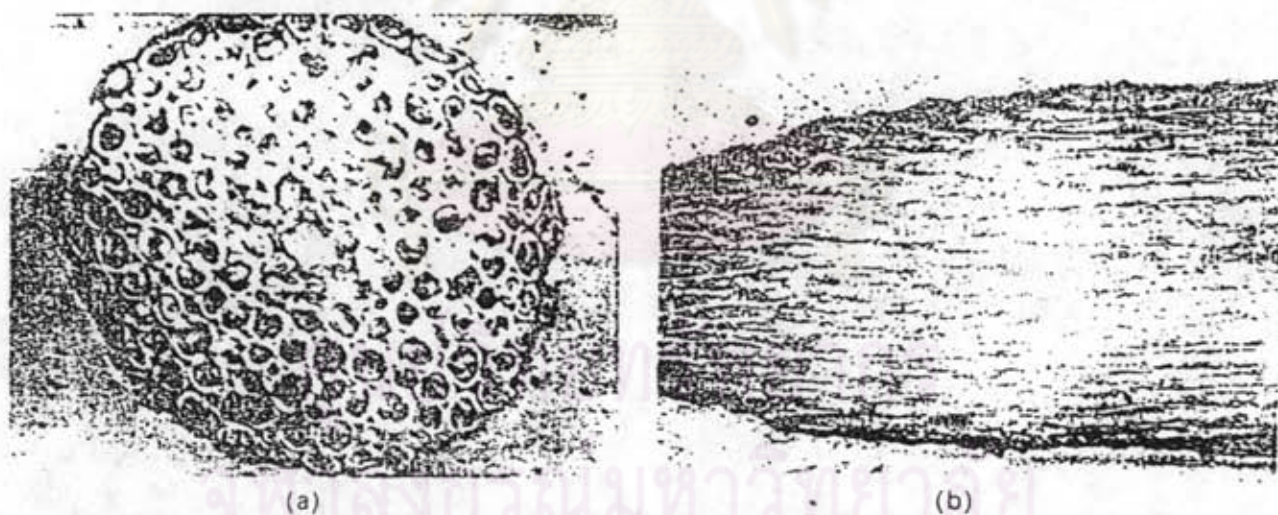


Figure 4.1 Typical microstructure of the coir fiber [(a)Cross-section of the coir fiber(x500); (b) Longitudinal of the fiber(x160)]

4.2 Kappa Number and Lignin Content of the Coir Fiber

The coir fiber was delignified by the treatment of 0.1 M NaOH at 100°C for 1, 2, 3, 4 and 5 hours. The delignified and original coir fiber

were determined in terms of the Kappa Number which could be transformed to lignin content by multiplying with a factor. The result is presented in Table 4.1:

Table 4.1 Relationship of Klason Lignin Content and Time of Treatment

Time to Treat (hour(s))	Weight of Sample (g)	Volume of Titrant (mL)	Kappa Number*		Klason*** Lignin Content (%)	Average (%)
			unadjustment (at 30 °C)	temperature correction** (at 25 °C)		
0	1.5349	15.90	46.20	49.41	7.41	7.45
	1.5036	16.23	46.63	49.87	7.48	
	1.5811	14.86	46.42	49.65	7.45	
1	2.0398	11.26	40.29	43.09	6.46	6.50
	2.0398	11.23	40.64	43.47	6.52	
	1.9024	13.29	40.57	43.39	6.51	
2	1.8807	10.05	42.35	45.29	6.79	6.38
	1.8154	15.31	37.25	39.84	5.98	
	1.8524	12.66	39.73	42.49	6.37	
3	2.0190	12.65	39.00	41.71	6.26	6.29
	1.7959	15.94	39.43	42.17	6.33	
	2.0314	12.28	39.22	41.95	6.29	
4	1.8807	15.55	38.15	40.80	6.12	6.09
	1.8154	16.93	37.72	40.34	6.05	
	2.0245	13.45	37.93	40.57	6.09	
5	2.0381	13.24	37.93	40.57	6.09	6.06
	2.0384	13.54	37.58	40.19	6.03	
	2.0368	13.38	37.79	40.42	6.06	

* Kappa Number could be calculated by equation as follows:

$$K = pxf/w \quad \text{-----(4.1)}$$

and

$$p = (b-a)N/0.1 \quad \text{-----(4.2)}$$

where

K = Kappa Number,

f = factor for correction to a 50% permanganate consumption, depending on the value of p, based on the equation:

$$\log K = \log P/W + 0.00093(p-50). \quad \text{-----}(4.2a)$$

** Correction for the reaction temperature: If the reaction did not occur at 25°C. The correct Kappa number was calculated from the following equation:

$$K = pf[1 + 0.013(25-t)]/w \quad \text{-----}(4.3)$$

where

t = actual reaction temperature in degrees Celsius.

*** Relationship with lignin: The Kappa Number gives essentially a straight line relationship with Klason Lignin. The percentage of Klason Lignin approximately equals to $K \times 0.15$.

4.3 Relationship of Lignin Content and Tensile Strength of the Coir Fiber

The lignin content of the coir fiber seemed to affect its tensile properties. The less lignin content, the higher tensile strength, but the variation of tensile strength was rather big because of the great variation in diameter of the coir fiber which was used to calculate the stress, the larger the diameter, the greater the tensile load.

The tensile strength at yield and strain of the coir fiber at any levels of the lignin content are shown in Table 4.2.

Table 4.2 Relationship of Klason Lignin Content(%) and Tensile Properties

Klason lignin content(%)	Tensile Strength(MPa)	Tensile Strain(%)
7.45	82.20	36.04
6.50	111.71	36.76
6.38	122.36	37.95
6.29	124.99	31.06
6.09	159.56	47.78
6.06	107.92	38.13

The microfibril of cellulose in the cell wall of the coir fiber was fused together by lignin. Delignification of lignin permits the microfibril of the coir fiber to be free from lignin which makes the coir fiber to become a spiral multi-fibril rope with stronger modulus.

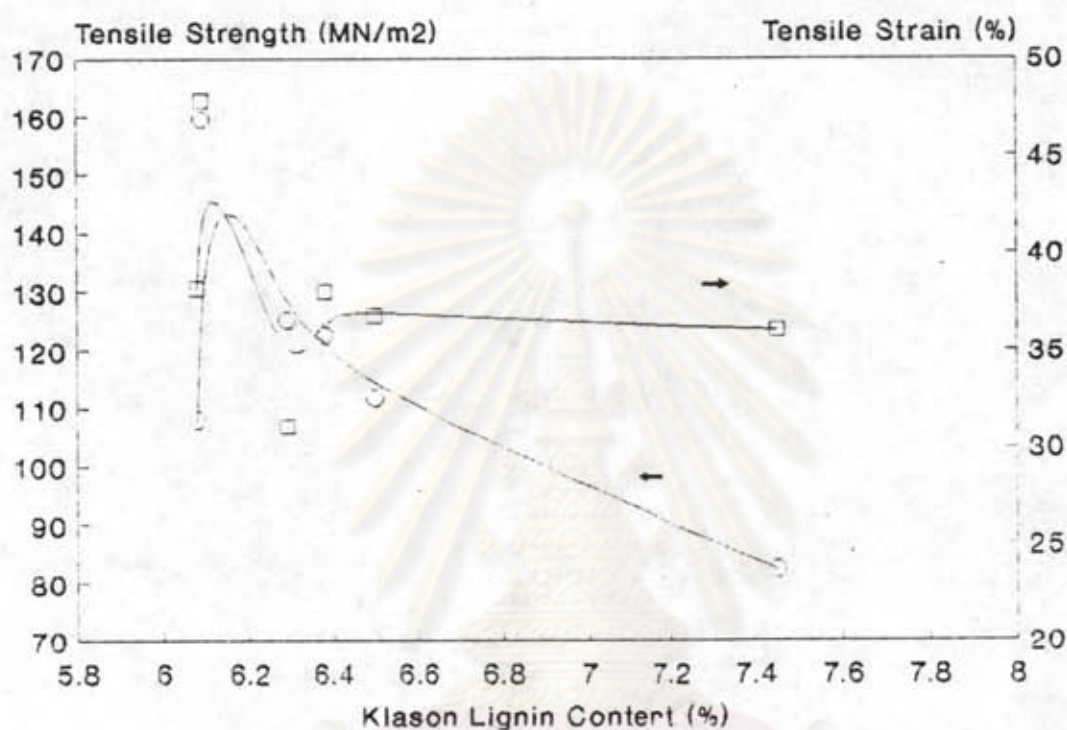
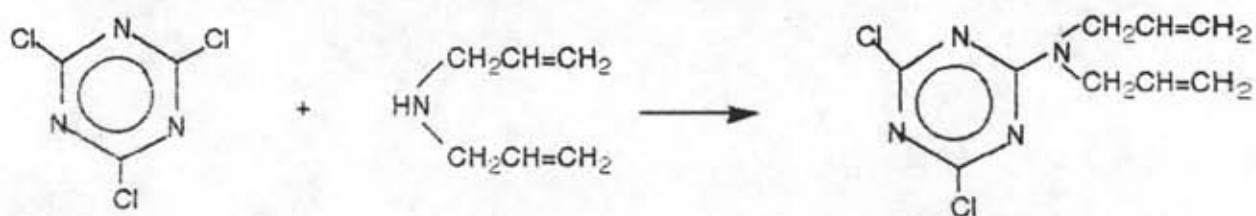


Figure 4.2 Relationship of Klason lignin content and tensile properties

4.4 2-Diallylamino-4,6-dichloro-s-triazine, the Coupling Agent

Since the coupling agent was synthesized from the nucleophilic reaction of 2,4,6-trichloro-s-triazine (cyanuric chloride) and diallylamine, the overall reaction can be shown by equation(4.1).



Cyanuric chloride

Diallyl amine

2-Diallylamino-4,6-dichloro-s-triazine, the coupling agent

The coupling agent has a melting point at 42°C. Percent yield was 85%.
The FT-IR spectrum was showed in Figure 4.3.

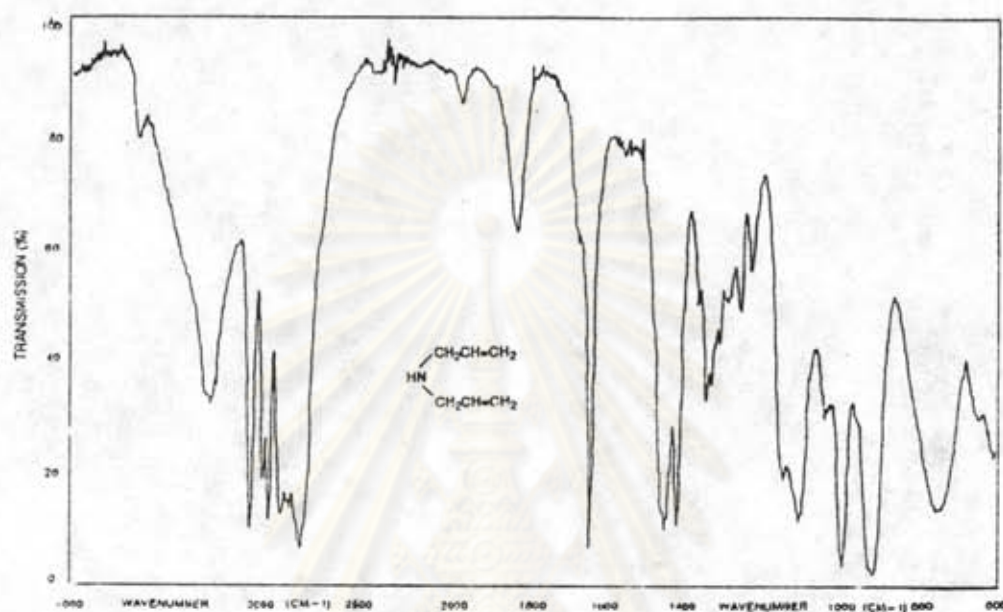


Figure 4.3 IR spectrum of diallyl amine

Table 4.3 Assignments of the IR Spectrum of Diallyl Amine

Assignments	Intensity	Wave Number (cm ⁻¹)
N-H stretch	medium	3280
C-H allyl stretch	strong	3070, 3010
C-H aliphatic stretch	strong	2980, 2900
C=C allyl stretch	weak	1640
C-N stretch	strong	1150

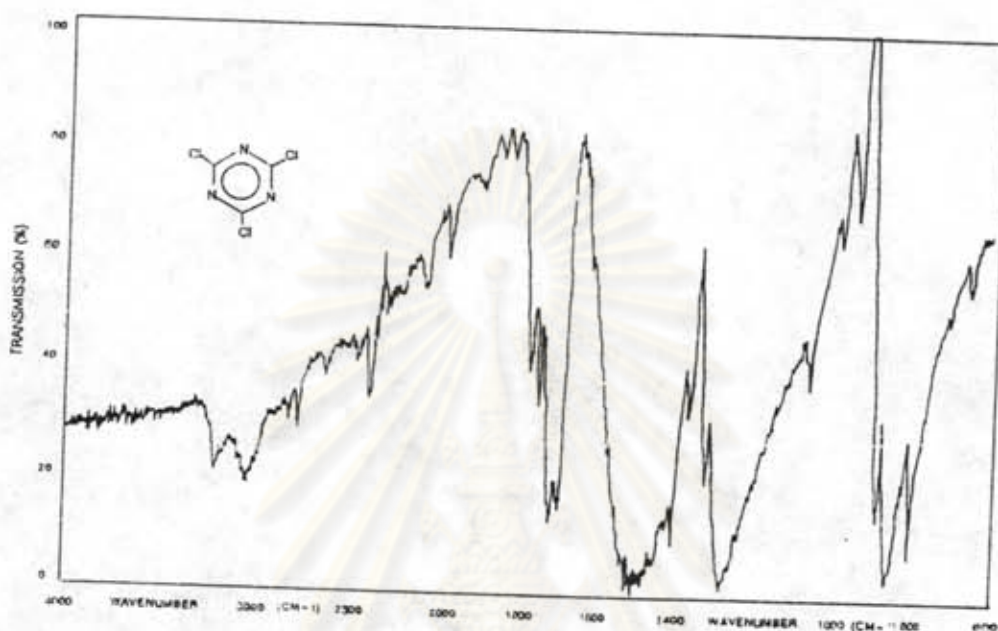


Figure 4.4 IR spectrum of cyanuric chloride

Table 4.4 Assignments of the IR Spectrum of Cyanuric Chloride

Assignments	Intensity	Wave Number (cm ⁻¹)
C=N s-triazine stretch	strong	500, 1275
C-Cl stretch	strong	880, 850, 795

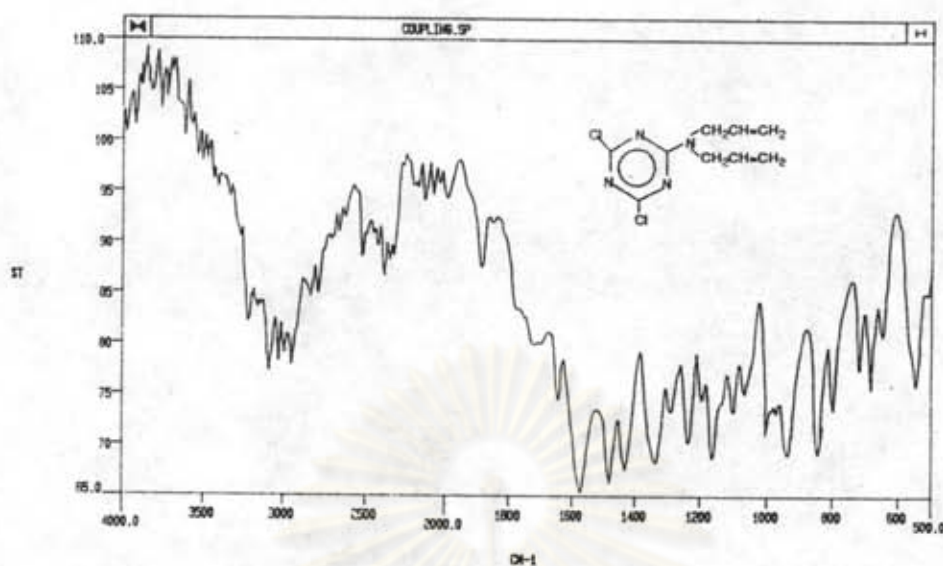


Figure 4.5 FT-IR spectrum (diffuse reflectance technique) of the coupling agent

Table 4.5 Assignments of the FT-IR Spectrum of the Coupling Agent

Assignments	Intensity	Wave Number (cm ⁻¹)
C-H alkene stretch	strong	3083 3025
C-H aliphatic stretch	strong	2990, 2941
C=C vinyl stretch	strong	1645
C=N s-triazine ring stretch	strong	1568
C-H aliphatic asym. bending	strong	1430
C-H aliphatic sym. bending	strong	1333
C-N stretch	strong	1285
C-Cl aromatic-attach stretch	strong	1099

From the infrared spectrum, the product showed the C=C absorption band at 1645 cm⁻¹ and the C=N absorption band at 1568 cm⁻¹ which were similar to those in the spectra of the starting materials, cyanuric chloride and diallylamine. In addition, the product showed a new absorption band at 1285 cm⁻¹ due to the C-N stretching. It is clear that the product contains the diallylamino group and triazine ring.

4.5 Detection of the Coupling Reaction between the Coir Fiber Surface and Unsaturated Polyester

Diffuse reflectance was originally developed for use in UV/visible spectroscopy, but ever since it has also become a widely used technique in FT-IR analysis. It is commonly used for : 1)powders, 2) solids that can be ground or scraped with abrasive paper, 3)the direct analysis of pellet. It has the advantages that no pressing is required and a wider array of samples can be analyzed.

With the FT-IR diffuse reflectance, a beam of infrared radiation reflects in a diffusely scattering manner by penetrating as shown in Figure 4.6.

The other part of the radiation, the specular component, reflects directly off the sample surface. The optics collects the scatter radiation and directs it to the infrared detector.

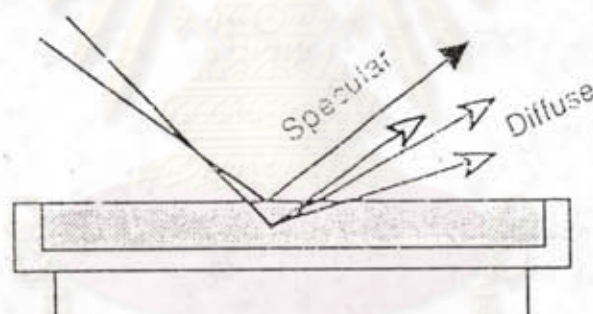


Figure 4.6 Diffuse vs. specular components in the diffuse reflectance spectroscopy

The other part of the radiation, the specular component, reflects directly off the sample surface. The optics collects the scatter radiation and directs it to the infrared detector.

Spectra obtained by the diffuse reflectance technique often appear differently from normal transmission spectra. The peak intensities at higher wavelengths tend to have decreased intensities relative to comparable transmission spectra and the peaks are not as sharp. For this reason, the spectra are usually transformed into Kubelka-Munk units, which have functions to compensate for these differences.

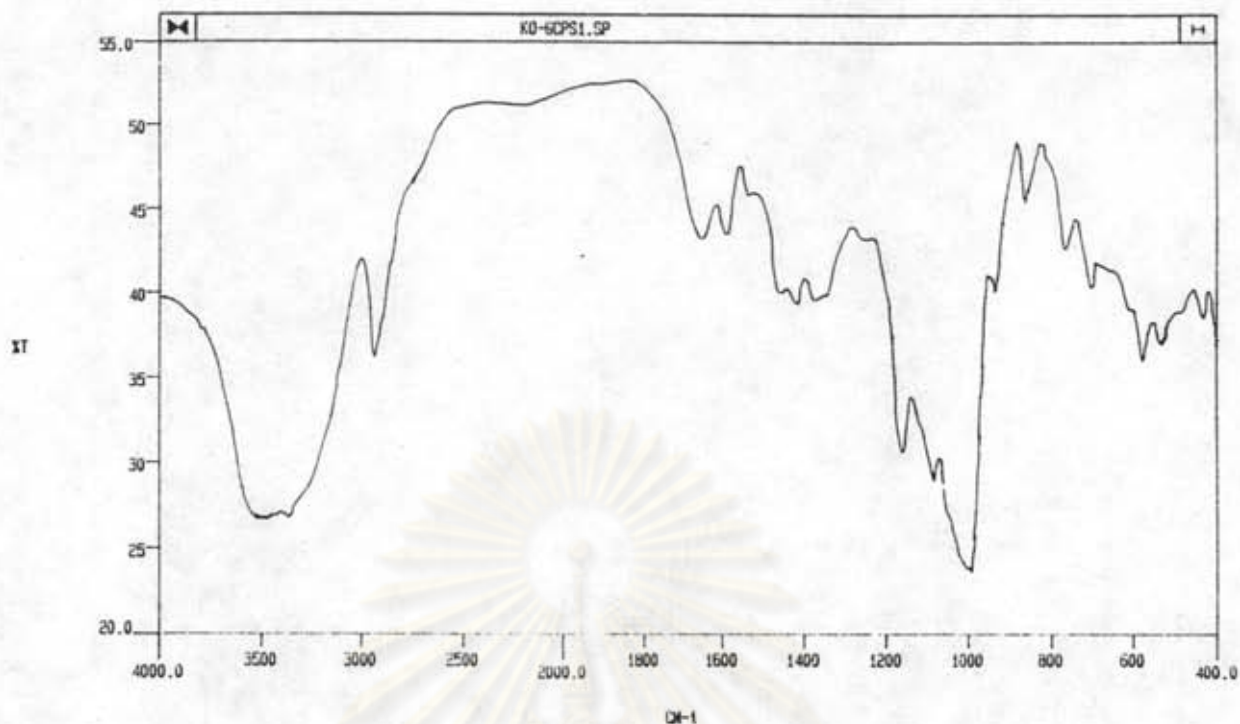


Figure 4.7 FT-IR (diffuse reflectance technique) spectrum of the surface of untreated coir powder.

This IR spectrum was similar to the pure cellulose IR spectrum. Therefore, the spectrum suggests that the coir fiber surface should comprise a lot of cellulose.

Table 4.6 Assignments of the FT-IR Spectrum of the Coir Powder

Assignments	Intensity	Wave Number (cm ⁻¹)
C-H intermolecular H-bonding broad band	strong	3800-3080
C-H aliphatic stretch	strong	2931
C-O alcohol stretch	strong	1083
C-O-C asym. stretch	strong	1160

The absorption bands at $3800\text{-}3080\text{ cm}^{-1}$ of the O-H intermolecular H-bonding, 1083 cm^{-1} of C-O alcohol stretch and 1160 cm^{-1} of the C-O-C asymmetric stretch confirmed that major constituent of the coir fiber surface is the cellulose.

4.5.1 The Coupling Reaction of the Coupling Agent onto the Coir Fiber Surface

The differential diffuse reflectance technique FT-IR of the coupling agent coated onto the coir powder surface and untreated coir powder obviously demonstrates the s-triazine peak (1567 cm^{-1})⁽¹⁸⁾ and the weak C=C absorption peak of the coupling agent (1640 cm^{-1}). It's certain that the coupling agent detected by FT-IR is chemically bonded to the coir powder since all of the unreacted coupling agent were removed by soxhlet extraction for 24 hours. Figure 4.8 illustrates the simplified molecular structure of the coir powder treated with the coupling agent. Many peaks above 3000 cm^{-1} in Figure 4.9 are the N-H stretching and other peaks are caused by direct reflectance (specular reflectance), since the more the wave number, the more the specular reflectance of the IR radiation.

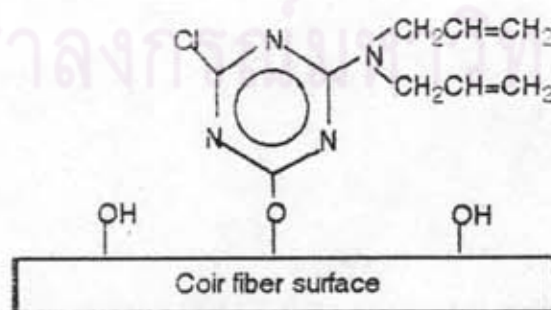


Figure 4.8 The simplified molecular structure of the coir powder treated with the coupling agent

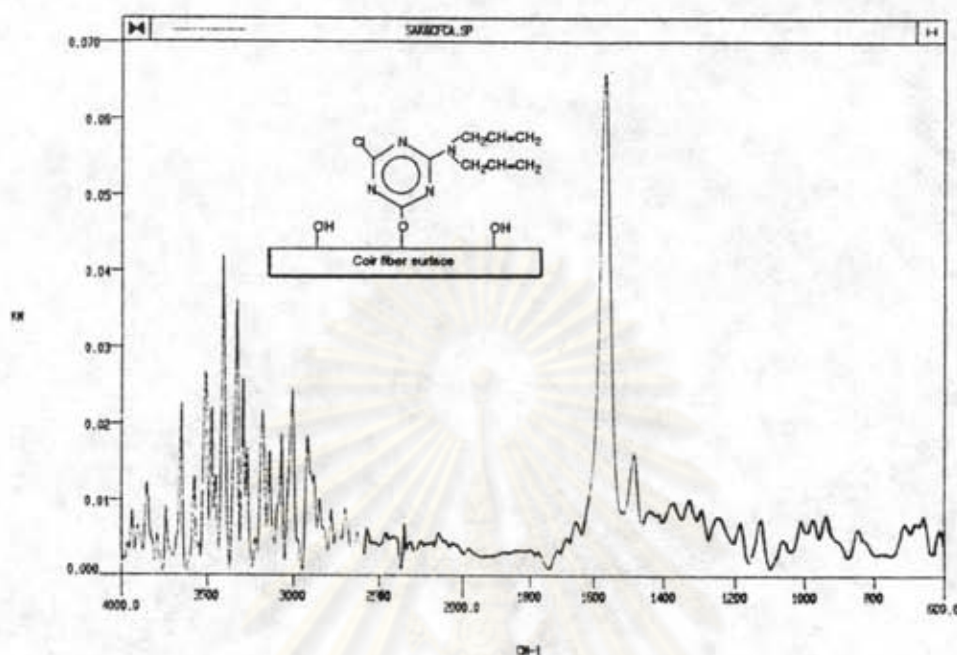


Figure 4.9 FT-IR (differential diffuse reflectance technique) spectrum of the coir powder treated with the coupling agent subtracted from the spectrum of the untreated coir powder

Table 4.7 Assignments of the FT-IR of the Coir Fiber Treated with the Coupling Agent

Assignments	Intensity	Wave Number (cm ⁻¹)
C-H alkene stretch	medium	3062, 3004
C-H aliphatic stretch	medium	2919
C=C vinyl stretch	weak	1640
C=N s-triazine ring stretch	strong	1567

The appearance of the s-triazine ring absorption band at 1567 cm⁻¹ and the C=C vinyl stretch band at 1640 cm⁻¹ may be the coupling reaction of the coupling agent onto the coir powder surface.

4.5.2 Copolymerization of the Coupling Agent and Styrene

There is no literature by far that indicates the existence of the copolymerization reaction of 2-diallylamino-4,6-dichloro-s-triazine and styrene. Verification of the existence of the coupling agent copolymerized with styrene monomer is essential. Such a polymerization reaction is shown in Figure 4.10. After the removal of polystyrene homopolymer by soxhlet extraction with toluene from the copolymer, the copolymer was confirmed by FT-IR (Figure 4.11). The peaks of s-triazine and styrene are present to confirm that styrene and s-triazine are the components of the copolymer.

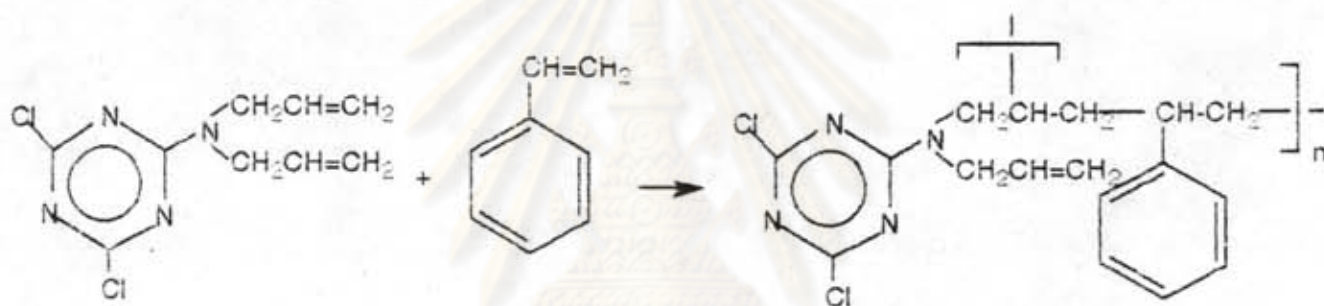


Figure 4.10 The copolymerization reaction of styrene monomer and the coupling agent

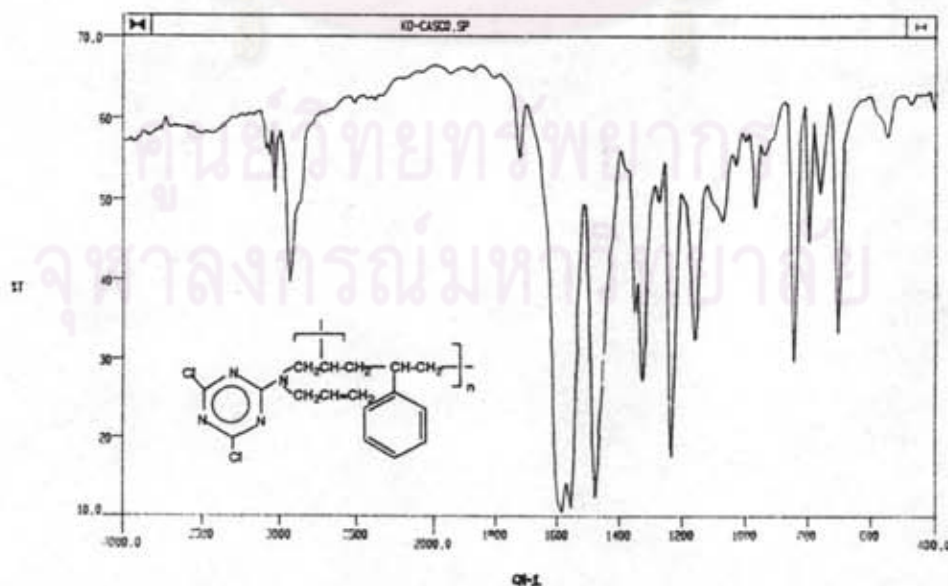


Figure 4.11 FT-IR spectrum of 2-diallylamino-4,6-dichloro-s-triazine-styrene copolymer

Table 4.8 Assignments of the FT-IR Spectrum of the Coupling Agent-Styrene Copolymer

Assignments	Intensity	Wave Number (cm ⁻¹)
C-H aromatic stretch	strong	3026
C-H aliphatic stretch	strong	2927
C=C aromatic ring stretch	strong	1551, 1474
C=N s-triazine ring stretch	strong	1583
C-H aliphatic asym. bending	medium	1347
C-H aliphatic sym. bending	medium	1324
C-N stretch	strong	1231

The absorption peaks at 3026 cm⁻¹ of the C-H aromatic, and at 1551, 1474 cm⁻¹ of the C=C aromatic ring stretch indicate that styrene was a part of the copolymer. The absorption peaks at 1583 cm⁻¹ of s-triazine ring stretch and at 1231 cm⁻¹ of C-N stretch confirm that the coupling agent was a part of the copolymer.

4.5.3 Graft Copolymerization of Styrene Monomer to the Coir Powder Surface Treated with the Coupling Agent

This experimental work is a direct verification of chemical adhesion occurring at the interface between the coir fiber and unsaturated polyester matrix (as shown in Figure 4.12). The Styrene monomer grafts easily onto the coir powder treated with the coupling agent at 50°C for 1 hour with benzoyl peroxide as an initiator. Figure 4.13 shows the occurrence of the expected graft copolymerization. From the IR spectrum, Figure 4.12, the absorption peaks of the C-H aromatic stretch at 3031 cm⁻¹ and the C=C aromatic ring stretch at 1600, 1494 and 1450 cm⁻¹ indicated the occurrence of the polystyrene grafted on the coir powder surface treated with the coupling agent. The disappearance of the absorption peaks of s-triazine ring was due to the shielding by a lot of polystyrene molecules at the coir powder surface.

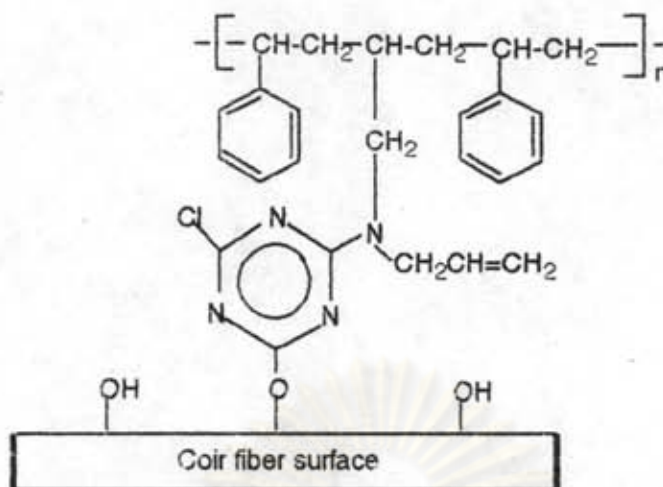


Figure 4.12 The simplified molecular structure of styrene monomer grafted onto the coir powder surface treated with the coupling agent

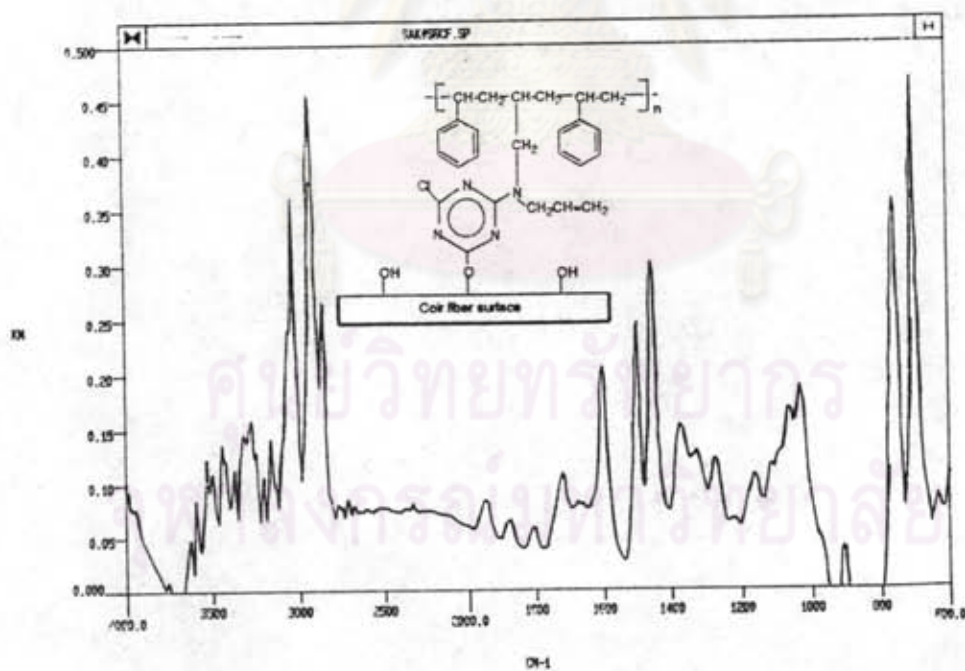


Figure 4.13 Diffuse reflectance technique of FT-IR of the graft copolymer of styrene onto the coir powder treated with the coupling agent.

Table 4.9 Assignments of the FT-IR Spectrum of Graft Copolymer of Styrene onto Coir Powder Treated with the Coupling Agent

Assignments	Intensity	Wave Number (cm ⁻¹)
C-H aromatic stretch	strong	3031
C-H aliphatic stretch	strong	2924, 2855
Overtone or combination bands	weak	1946, 1876, 1805
C=C aromatic ring stretch	strong	1600, 1494, 1450
C-H aliphatic asym. bending	medium	1371
C-H aliphatic sym. bending	medium	1310

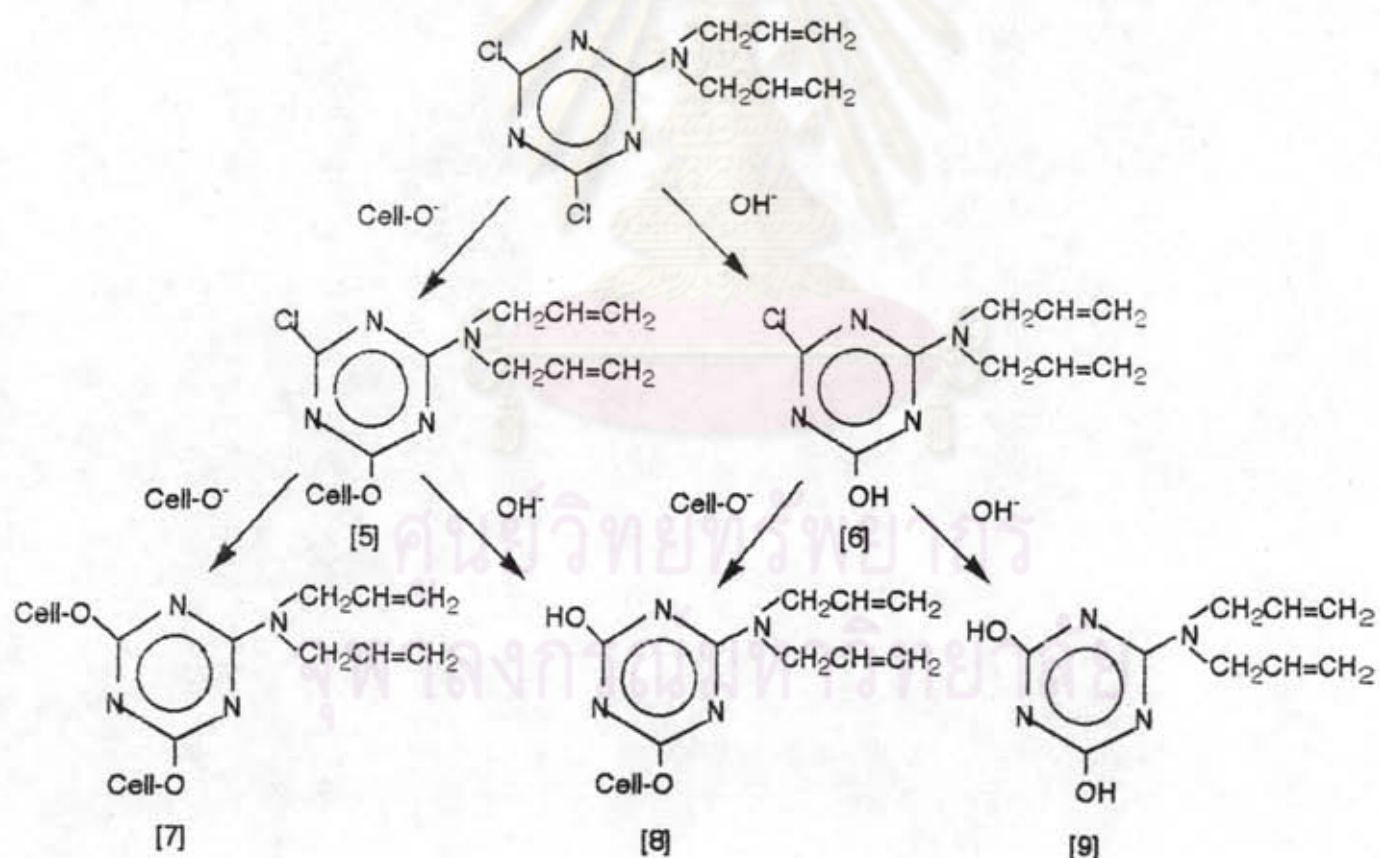


Figure 4.14 Possible structures of the coupling reaction between coir fiber surface and 2-diallylamino-4,6-dichloro-s-triazine

However the treatment of the coir fiber surface not only occurred the structure [5] but also could possibly occurred structures summarized in Figure 4.14. Compounds [6] and [9] was removed during washing and extraction of the fiber. What structures are the compound occurring on the coir fiber surface should be researched in the future.

4.6 Differential Thermal Analysis (DTA) of the Coir Fiber-UP

Composites

DTA thermographs of pure UP resin, untreated coir fiber and 8%-treated coir fiber-UP composites were shown in Figures 4.14a, 4.14b and 4.14c respectively. Glass transition temperature (T_g) of UP matrix was observed at 73°C in all thermographs. The thermograph of a pure UP resin gave a glass transition temperature at 73°C. In the presence of untreated coir fiber embedded in the UP matrix, the additional peak of melting transition temperature, T_m , of the coir fiber at 146°C (Figure 4.17) was observed. Additional transition peaks of T_m at 170°C and 187°C departed from 150°C were also observed in the presence of 8%-treated coir fiber embedded in the UP matrix which possibly belonged to the coupling reaction phase around the fiber.

4.7 Scanning Electron Microscopy (SEM) of the Coir Fiber-UP

Composites

Scanning electron microscopy was used to study the presence of the adhesion between the coir fiber and UP matrix at the impact fracture surface of the composite. Figure 4.15a1-Figure 4.15a9 show the lack of adhesion at the interface between the untreated coir fiber and the matrix, and the evidence of fiber pull-out due to the absence of chemical bond between this interface. The presence of micro fibrils linked between the fiber and the UP matrix, and the evidence of fiber fracture themselves (as shown in Figure 4.15b1-Figure 4.15b9) possibly indicated that in the 8%-treated coir fiber and the UP matrix, an adhesion between them occurred which was induced by the coupling reaction.

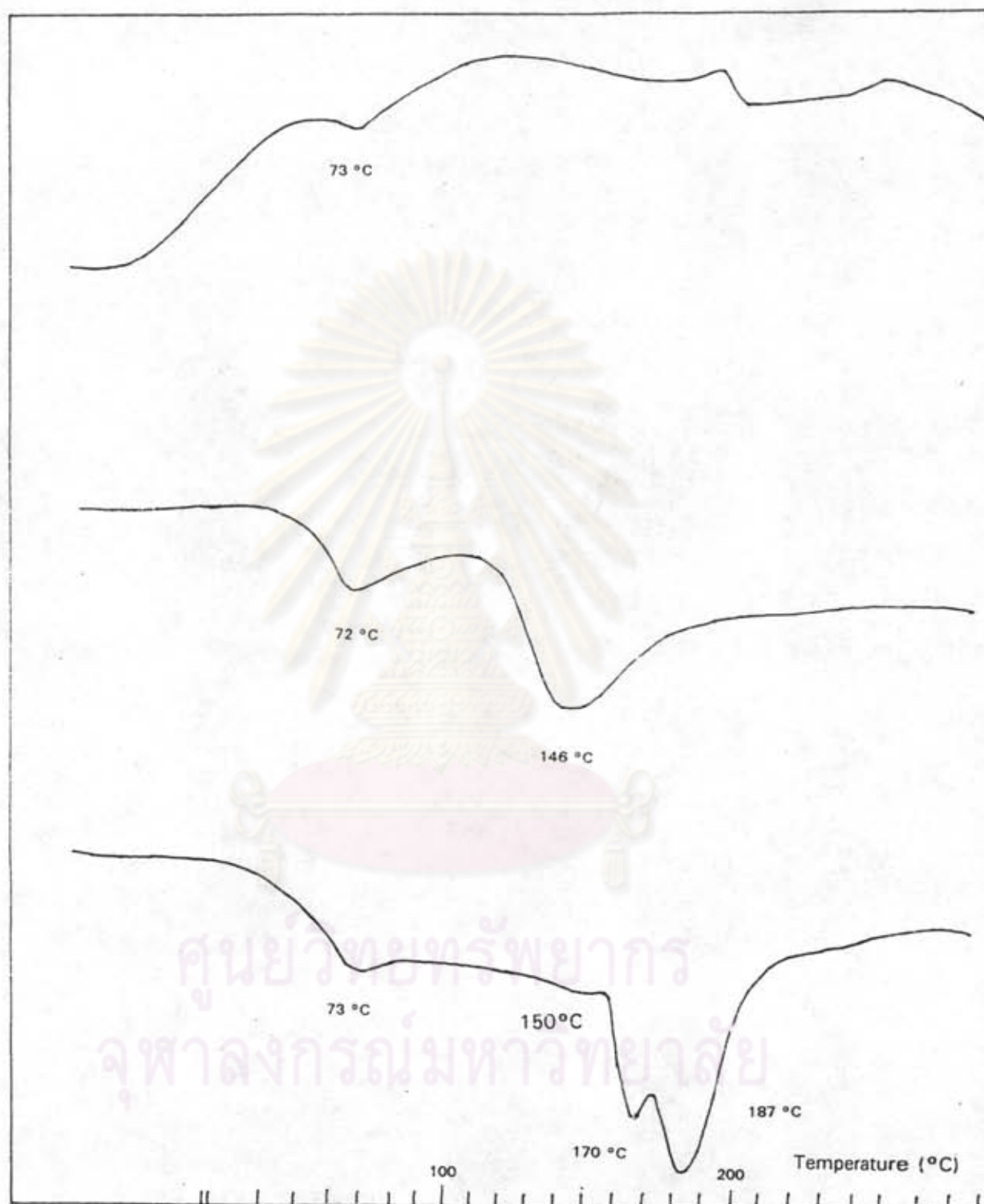
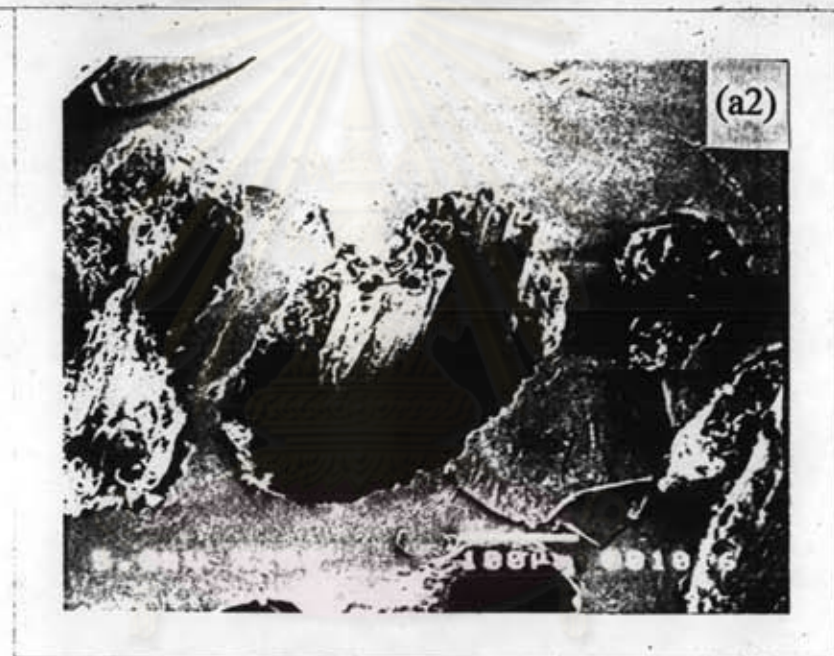
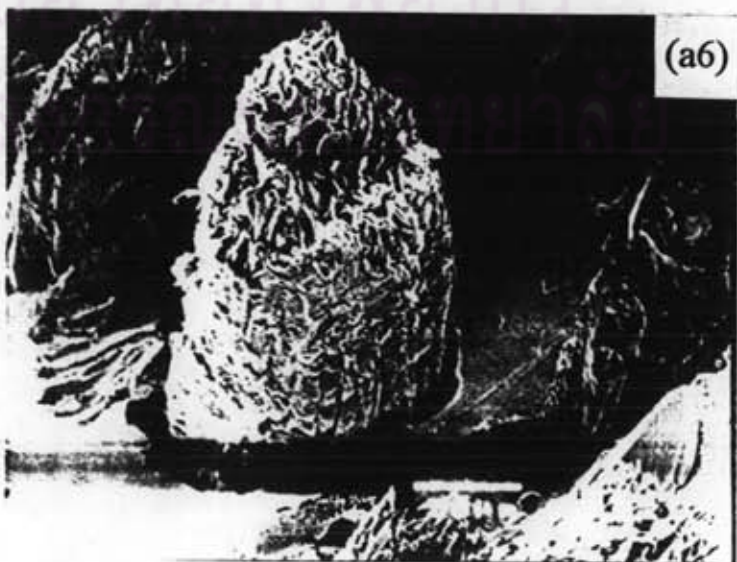
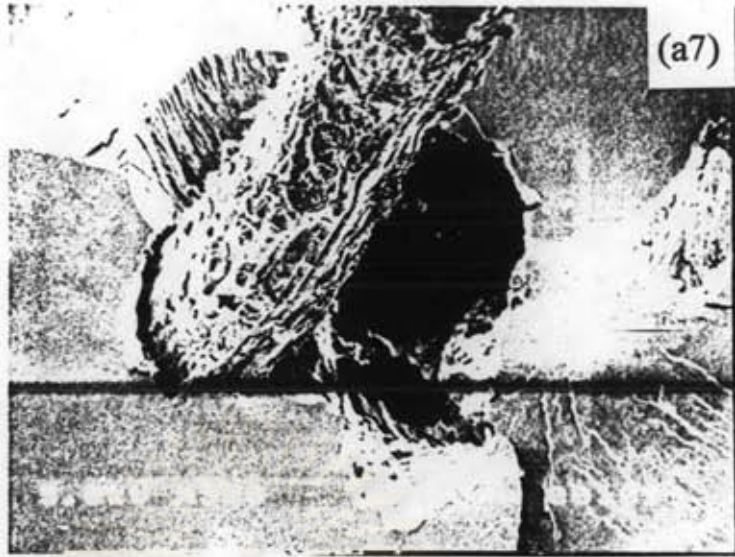
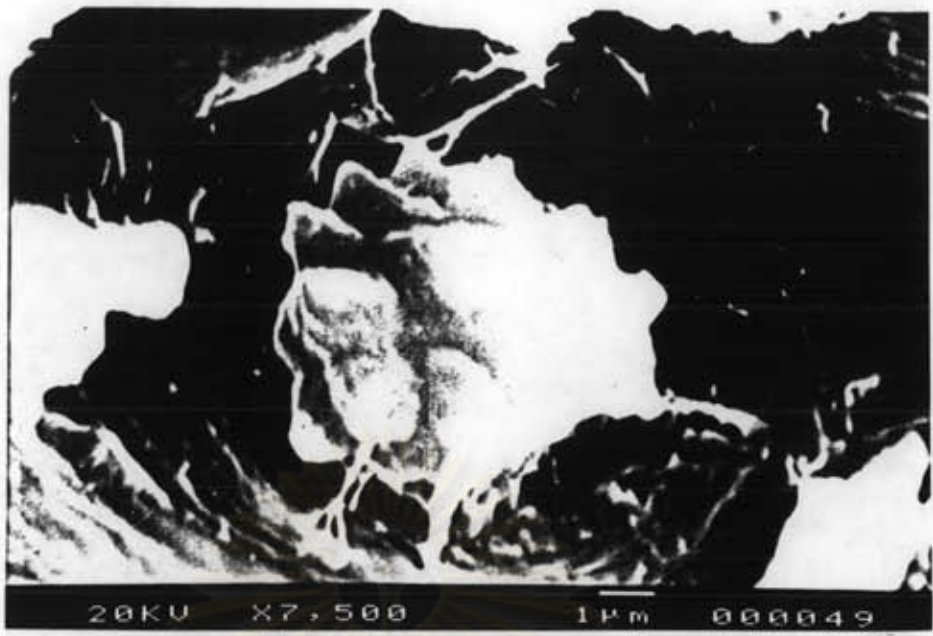


Figure 4.15 Differential Thermal Analysis Thermographs of pure UP resin (a), untreated coir fiber-UP composite (b) and 8%-treated coir fiber-UP composites (c).

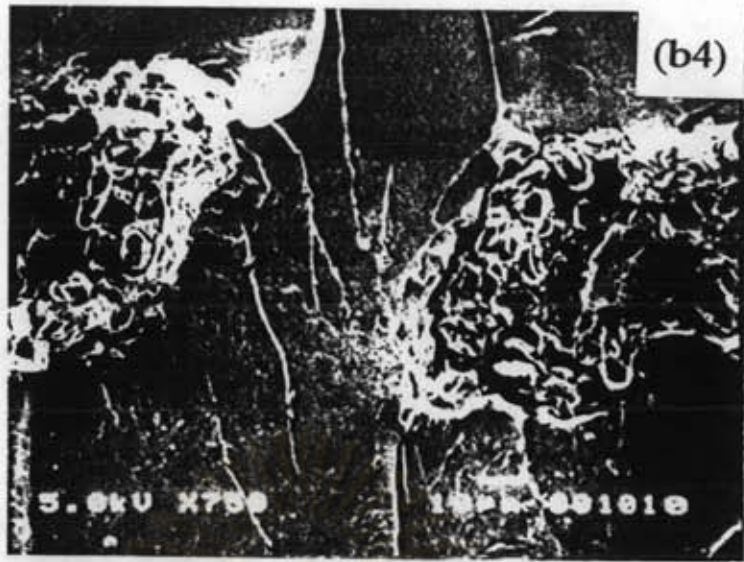








ศูนย์วิจัยทรัพยากร
จุฬาลงกรณ์มหาวิทยาลัย



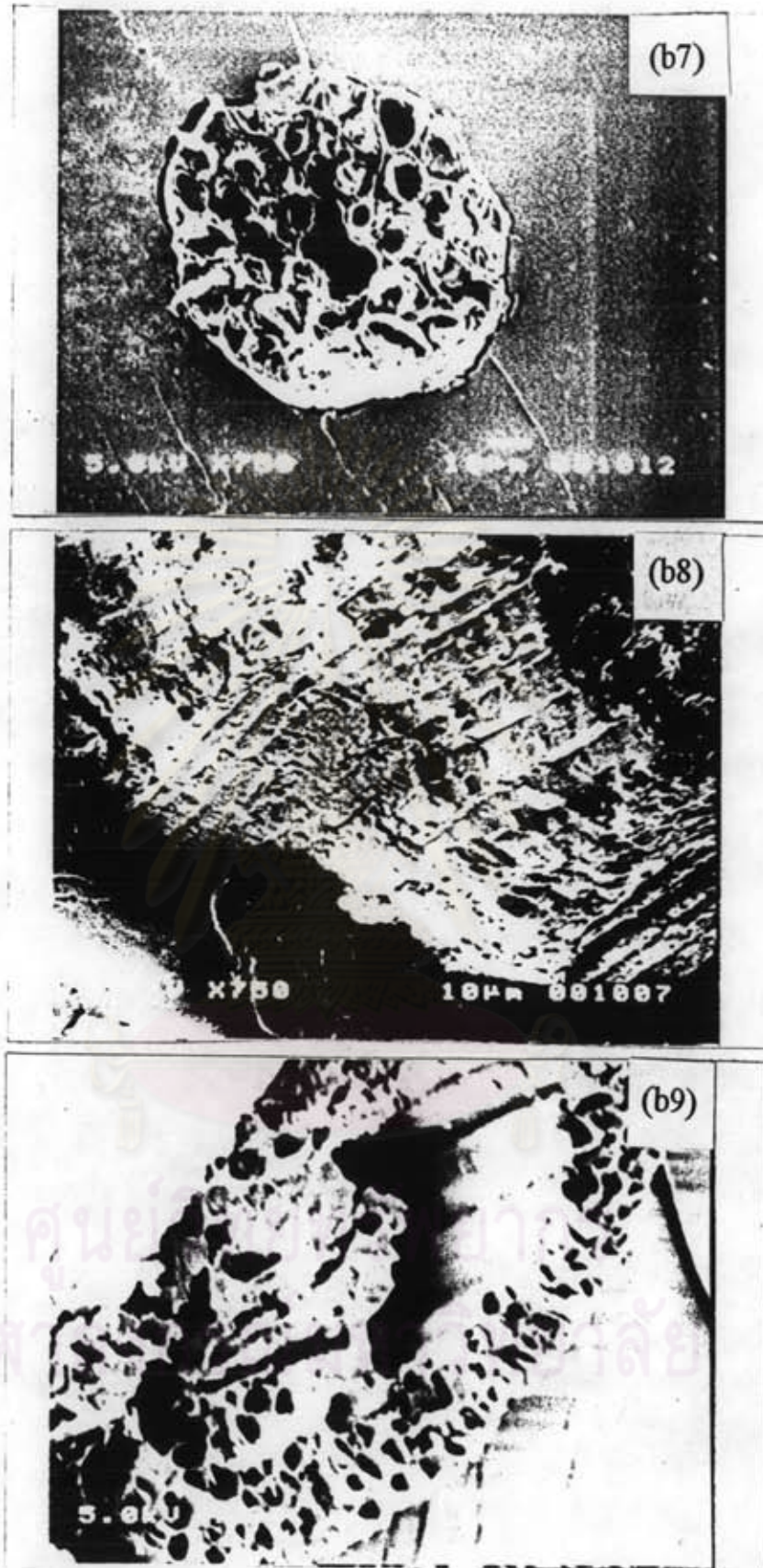


Figure 4.16 Scanning Electron Microscopy (SEM) of the impact fractured surface of untreated (a1-a9) and 8%-treated (b1-b9) coir fiber-UP composite.

4.8 Mechanical Properties of the Composites

Mechanical properties of the coir fiber-UP resin can indirectly indicate the performance behavior of the interfacial adhesion between the fiber and the matrix. The greater the interfacial adhesion, the better the mechanical properties. In this work, four types of mechanical properties were tested consisting of tensile properties, compressive properties, flexural properties and impact strength. To select materials for engineering design so as to fabricate any product one should know the proper properties for the respective functions and performance application.

4.8.1 Tensile Properties

Table 4.10 exhibits tensile properties of the coir fiber-UP resin composites at various conditions of the coir fiber. The results obviously indicate that the coir fiber reinforcement has a potential to increase tensile strength and modulus (as shown in Figures 4.16a and 4.16b) in the presence of the coupling agent. This fact indicates that there is a type of chemical bonding between the fiber and the matrix in such of the coupling agent. Indeed, in the absence of such bonding, the fiber would act as a void and therefore stress concentration exists, thereby it reduce the tensile strength and modulus of the specimens. In the absence of coupling agent, the appearance of interfacial adhesion may be due to solely the fiber wetting via physical absorption or secondary chemical bond, i.e., van der Waals force.

One possible failure mode of fiber reinforced composites is pull-out, which results from interfacial bond failure and a second mode is fiber fracture⁽⁵⁸⁾. In the presence and absence of the coupling agent, the corresponding composites showed fiber fracture in presence of use the coupling agent and partial fiber pull-out in the absence of the coupling agent. The tensile strength and modulus of the treated coir fiber composites are significantly higher than the untreated one because the ability to transfer a tensile load from the matrix to the fiber via chemical bond of the matrix-coupling agent was increased. The more concentration of the coupling agent treated on the coir fiber surface the

more chemical bond between interface. Figures 4.19a and 4.19b show the effect of the coir fiber length upon tensile properties of the composites. No significant improvement in tensile properties was obtained in all cases of the coir fiber length. Since fiber fracture instead of fiber pull-out is observed, there is no significant increase of the tensile strength and modulus with the fiber length due to that the fiber length is above the critical length, l_c (1 mm) calculated from the aspect ratio as shown below:

From equation 2.29

$$l_c/d = \sigma_f/2\tau$$

where

$\sigma = 160$ MPa (from Table 4.2),

$\tau = 20$ MPa (from Table 4.9),

$d =$ diameter of the coir fiber = 0.25 mm

Therefore, the l_c can be deduced from these values to give a value of 1 mm.

4.8.2 Compressive Properties

The compressive strength and modulus were increased with the addition of the coir fiber reinforcement (shown in Table 4.11, Figures 4.17a and 4.17b, respectively) because the fiber wetting via physical adhesion occurred. Lack of interfacial adhesion causes the decrease of both compressive strength and modulus because the fiber acts as a stress concentration. The composites consisting of the untreated coir fiber have the lower compressive strength and modulus than the treated ones. And so, the results imply that there is the interfacial bonding between the fiber and the matrix. Indeed, the increase in fiber wetting occurred from interfacial adhesion regardless of the type of force. In the case of the treated coir fiber, the interfacial bond was truly a chemical bonding resulted from the coupling reaction as showed in Figure 4.18.

The work of adhesion concerning two phase adherence can be calculated from equation below⁽⁶⁹⁾:

$$W_a = \gamma_1 + \gamma_2 - \gamma_{12} \quad \text{-----(4.1)}$$

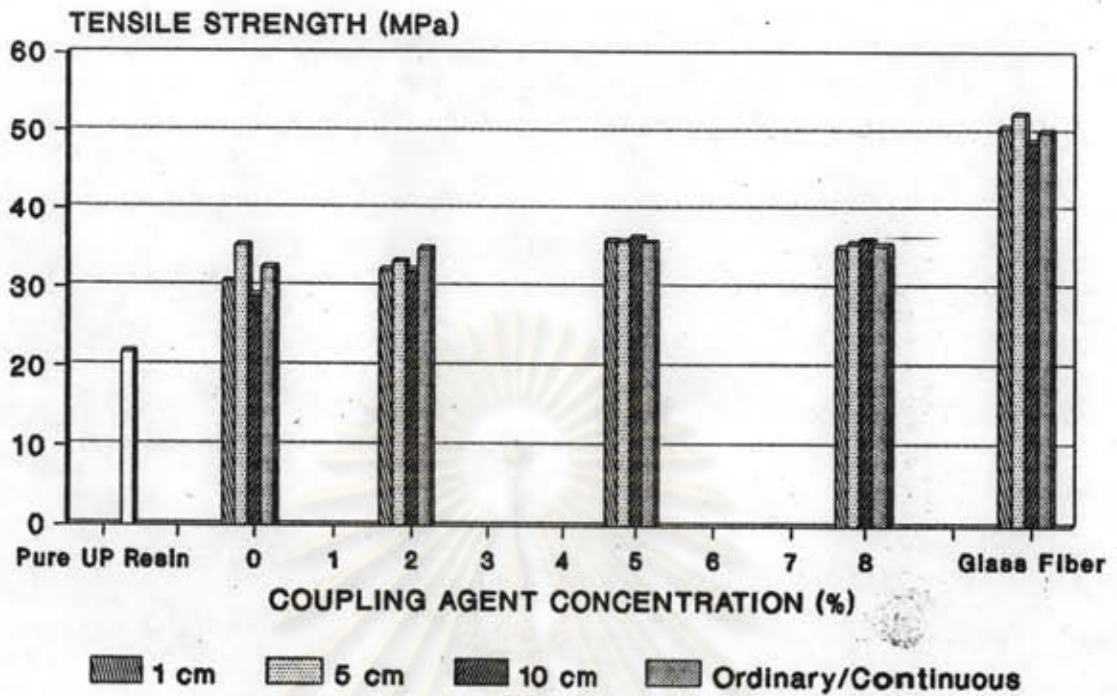
Table 4.10 Effect of the Coupling Agent on Tensile Properties of 20% Coir Fiber-UP Composites at Various Fiber Lengths

Sample	Fiber Length (cm)	[Coupling Agent] (%)	Tensile Strength (MPa)		Tensile Strain (%)		Young's Modulus (MPa)	
			S.D.*		S.D.		S.D.	
Pure UP Resin	-	-	21.71	2.78	0.69	0.07	3138	153
Coir Fiber-UP Resin	1	-	30.78	3.05	1.19	0.45	3418	151
Coir Fiber-UP Resin	5	-	35.30	5.50	1.09	0.24	3310	457
Coir Fiber-UP Resin	10	-	28.92	1.87	0.87	0.07	3233	241
Coir Fiber-UP Resin	Ordinary**	-	32.44	1.90	1.08	0.02	3695	241
Coir Fiber-UP Resin	1	2	32.15	0.72	0.92	0.00	3135	179
Coir Fiber-UP Resin	5	2	33.26	1.77	1.30	0.06	3432	163
Coir Fiber-UP Resin	10	2	32.17	1.16	1.31	0.72	3729	620
Coir Fiber-UP Resin	Ordinary	2	34.96	0.53	1.18	0.21	3291	222
Coir Fiber-UP Resin	1	5	35.99	2.24	1.04	0.28	3877	9
Coir Fiber-UP Resin	5	5	35.84	1.58	1.08	0.33	3876	12
Coir Fiber-UP Resin	10	5	36.42	1.73	1.05	0.17	3876	12
Coir Fiber-UP Resin	Ordinary	5	35.79	1.32	0.93	0.13	3874	14
Coir Fiber-UP Resin	1	8	35.14	1.26	0.94	0.08	3879	13
Coir Fiber-UP Resin	5	8	35.69	1.55	1.04	0.09	3901	13
Coir Fiber-UP Resin	10	8	36.19	1.03	1.13	0.15	3901	8
Coir Fiber-UP Resin	Ordinary	8	35.39	0.87	0.95	0.03	3901	13
Glass Fiber-UP Resin	1	-	50.60	3.01	0.65	0.08	8301	219
Glass Fiber-UP Resin	5	-	52.26	4.11	0.56	0.08	9887	83
Glass Fiber-UP Resin	10	-	48.78	5.34	0.55	0.10	11040	72
Glass Fiber-UP Resin	Continuous***	-	50.10	8.65	0.61	0.16	11060	88

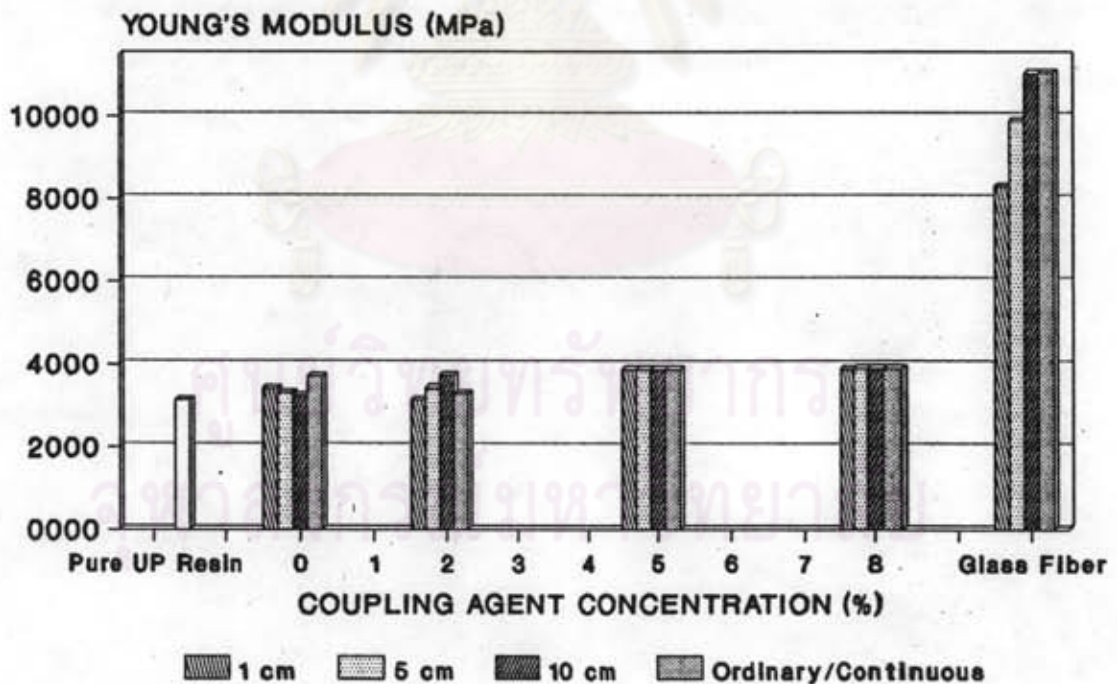
* Standard deviation

** Ordinary length of the coir fiber

*** Continuous glass fiber length



(a)



(b)

Figure 4.17 Effect of the coupling agent and coir fiber length on tensile properties [(a)Tensile strength, (b)Young's modulus]

where

W_a = work of adhesion,

γ_1 = surface tension of phase 1,

γ_2 = surface tension of phase 2,

γ_{12} = interfacial tension between phases 1 and 2.

The value of shear strength used to separate two phases apart is directly proportional to the work of adhesion, W_a . Thus, the treatment of the coir fiber with the coupling agent increased the work of adhesion or on the other hand, it particularly reduced the value of interfacial tension, γ_{12} . It means that shear strength of the composites increased in relation to the work of adhesion. A slight increase in compressive strength and modulus was also observed from 2% to 8% treated coir fiber composites. There was not significant difference in compressive strength and modulus at any coir fiber length in each category because the fiber length was greater than their critical length, about 1 mm (Section 3.3.10). The behavior that makes the treated coir fiber composites having better compressive properties is the more interfacial adhesion induced by more chemical bonds resulted from the coupling reaction.

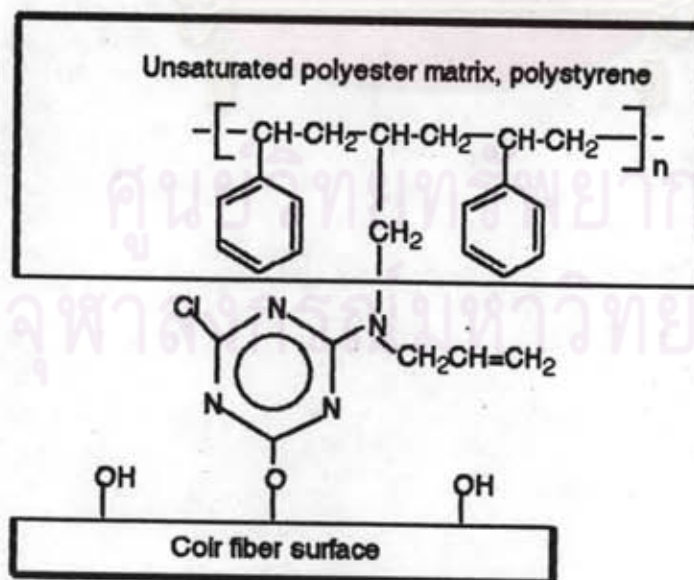


Figure 4.18 Interfacial bond induced by the coupling reaction

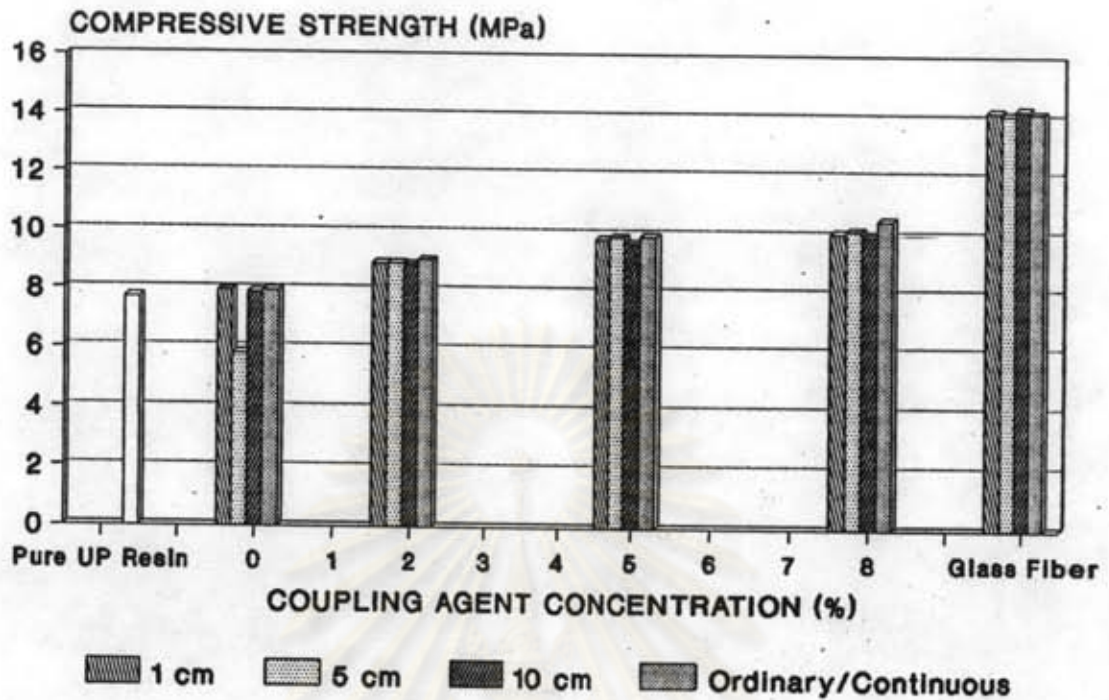
Table 4.11 Effect of the Coupling Agent on Compressive Properties of 20% Coir Fiber-UP Composites at Various Fiber Lengths

Sample	Fiber Length (cm)	[Coupling Agent] (%)	Compressive Strength (MPa)		Compressive Strain (%)		Modulus of Elasticity (MPa)	
			S.D.*		S.D.		S.D.	
Pure UP Resin	-	-	7.71	2.44	1.19	0.41	1818	824
Coir Fiber-UP Resin	1	-	7.93	0.45	0.62	0.13	1850	3
Coir Fiber-UP Resin	5	-	5.82	0.52	0.88	0.40	1870	32
Coir Fiber-UP Resin	10	-	7.88	0.20	0.56	0.51	1807	60
Coir Fiber-UP Resin	Ordinary**	-	7.96	1.33	0.84	0.16	1842	43
Coir Fiber-UP Resin	1	2	8.90	0.48	0.82	0.21	1920	92
Coir Fiber-UP Resin	5	2	8.90	0.22	0.68	0.30	1876	81
Coir Fiber-UP Resin	10	2	8.87	0.13	1.34	0.36	1893	60
Coir Fiber-UP Resin	Ordinary	2	9.02	0.22	1.10	0.64	2047	126
Coir Fiber-UP Resin	1	5	9.76	0.33	0.52	0.30	1859	33
Coir Fiber-UP Resin	5	5	9.85	0.38	0.67	0.39	1970	127
Coir Fiber-UP Resin	10	5	9.64	0.37	0.74	0.24	1910	133
Coir Fiber-UP Resin	Ordinary	5	9.88	0.24	1.23	0.44	1951	8
Coir Fiber-UP Resin	1	8	10.02	0.21	0.64	0.36	1986	64
Coir Fiber-UP Resin	5	8	10.10	0.58	1.02	0.35	2223	164
Coir Fiber-UP Resin	10	8	9.92	0.56	1.81	0.52	2052	10
Coir Fiber-UP Resin	Ordinary	8	10.44	0.51	0.71	0.35	2053	24
Glass Fiber-UP Resin	1	-	14.20	0.53	0.61	0.38	3505	18
Glass Fiber-UP Resin	5	-	14.10	0.38	1.00	0.32	3920	351
Glass Fiber-UP Resin	10	-	14.28	0.67	0.61	0.35	3557	9
Glass Fiber-UP Resin	Continuous***	-	14.16	0.83	1.02	0.42	3568	3

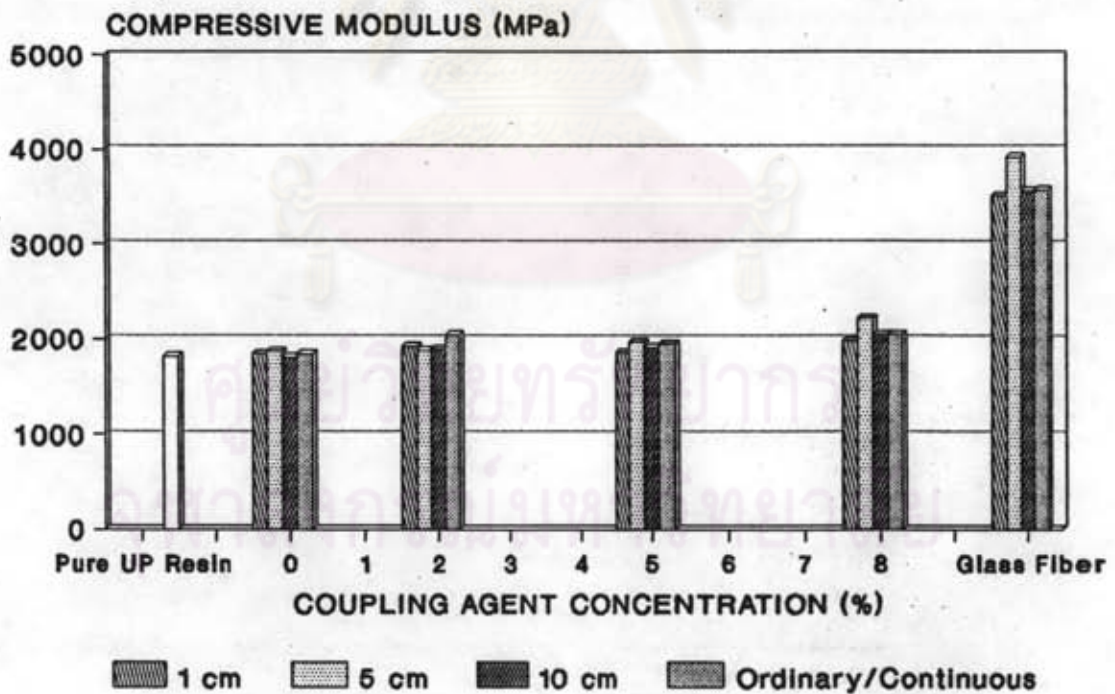
* Standard deviation

** Ordinary length of the coir fiber

*** Continuous glass fiber length



(a)



(b)

Figure 4.19 Effect of the coupling agent and coir fiber length on compressive properties [(a)Compressive strength, (b)Compressive modulus]

4.8.3 Flexural Properties

The flexural strength and modulus of the coir fiber composites are higher than those of the pure UP resin. Treatment of the coir fiber with the coupling agent in composites gives better flexural strength and modulus than the untreated one (Figures 4.19a and 4.19b). An increase in the coupling agent concentration for treatment of the coir fiber increases both the flexural strength and modulus. The length of the coir fiber does not impose any changes in flexural strength and modulus of the composites. Table 4.12 shows the flexural properties of the composites. It may be noted that chemical adhesion between the fiber and the matrix induces significantly better flexural properties.

4.8.4 Impact Resistance

The result from Table 4.13 shows that the coir fiber reinforcement can increase impact strength and especially, the treated coir fiber with the coupling agent, 2-diallylamino-4,6-dichloro-s-triazine, can improve the more impact strength than the untreated ones. In addition, the impact strength of any composites will increase by addition with more ductile additives in the matrix. The ductility of the additives will act as a crack stopper as described in Section 2.1.4.1.b.3. Thus, the impact strength of coir fiber-UP resin composites is increased by the more ductility of the coir fiber. Indeed, the mechanisms of fracture toughness occurred in two ways; first, the tip of crack growth was stopped by the fiber which could absorb the total energy of surface fracture and second, the tip of crack growth changed the direction to form delamination of the fiber and the matrix in case of the surface fracture energy was greater than interfacial tension energy. Thus, an increase of coupling agent concentration to treat the coir fiber would increase the interfacial tension energy between the fiber and matrix. The result is the fracture toughness increases, so impact strength of 2%- to 8%-treated coir fiber composites would increase, respectively. The coir fiber length did not affect the impact strength of the composites at a specific coupling agent concentration as illustrated in Figure 4.20 because the capacity of

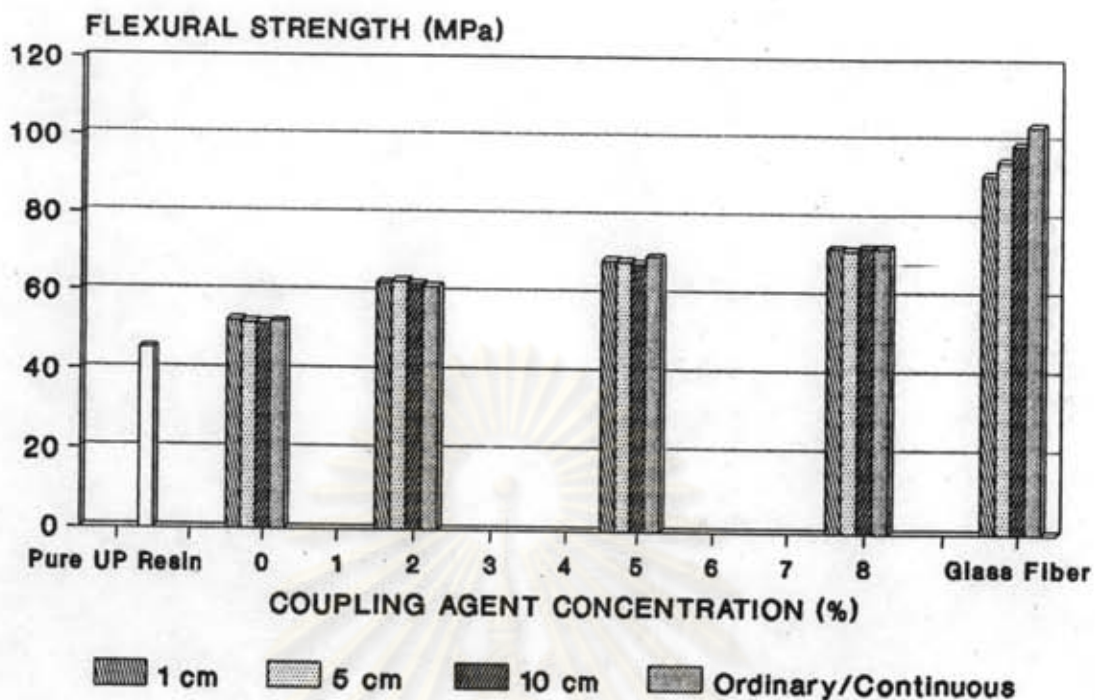
Table 4.12 Effect of the Coupling Agent on Flexural Properties of 20% Coir Fiber-UP Composites at Various Fiber Lengths

Sample	Fiber Length (cm)	[Coupling Agent] (%)	Flexural Strength (MPa)		Flexural Strain (mm/mm)		Modulus of Elasticity (MPa)	
			S.D.*		S.D.		S.D.	
Pure UP Resin	-	-	45.42	2.44	0.0192	0.0038	2611	824
Coir Fiber-UP Resin	1	-	52.63	0.58	0.0195	0.0021	3095	3
Coir Fiber-UP Resin	5	-	52.12	1.82	0.0221	0.0043	3069	16
Coir Fiber-UP Resin	10	-	51.85	0.52	0.0242	0.0043	2953	60
Coir Fiber-UP Resin	Ordinary**	-	52.19	1.84	0.0249	0.0086	2883	581
Coir Fiber-UP Resin	1	2	62.44	3.48	0.0199	0.0057	3164	92
Coir Fiber-UP Resin	5	2	62.94	0.79	0.0230	0.0048	3303	84
Coir Fiber-UP Resin	10	2	62.22	0.65	0.0286	0.0128	3170	60
Coir Fiber-UP Resin	Ordinary	2	61.52	2.22	0.0284	0.0071	3171	126
Coir Fiber-UP Resin	1	5	68.61	1.00	0.0276	0.0039	3140	33
Coir Fiber-UP Resin	5	5	68.32	1.76	0.0232	0.0033	3250	127
Coir Fiber-UP Resin	10	5	67.82	0.55	0.0271	0.0007	3330	189
Coir Fiber-UP Resin	Ordinary	5	69.55	0.74	0.0261	0.0045	3329	31
Coir Fiber-UP Resin	1	8	72.04	1.68	0.0223	0.0031	3300	12
Coir Fiber-UP Resin	5	8	71.58	1.26	0.0234	0.0029	3300	17
Coir Fiber-UP Resin	10	8	72.32	1.39	0.0261	0.0055	3166	299
Coir Fiber-UP Resin	Ordinary	8	72.15	1.28	0.0249	0.0034	3305	18
Glass Fiber-UP Resin	1	-	91.09	3.67	0.0219	0.0017	5833	554
Glass Fiber-UP Resin	5	-	94.69	5.87	0.0280	0.0111	5271	75
Glass Fiber-UP Resin	10	-	98.72	4.41	0.0213	0.0012	5499	2
Glass Fiber-UP Resin	Continuous***	-	103.60	3.10	0.0256	0.0054	5700	2

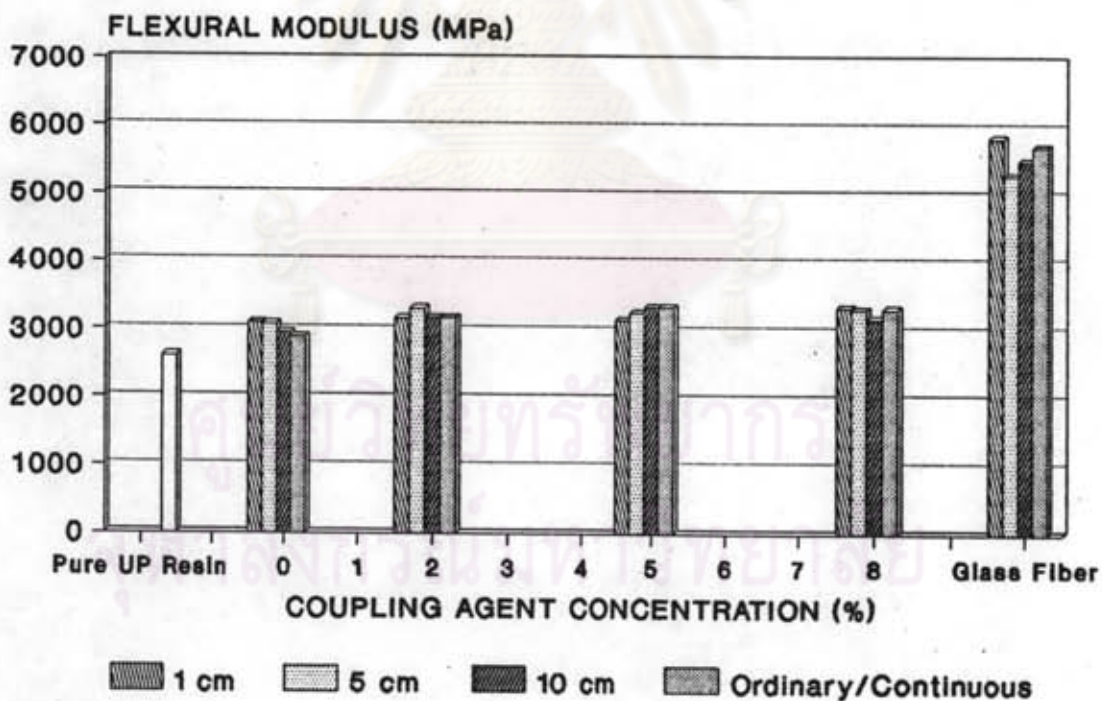
* Standard deviation

** Ordinary length of the coir fiber

*** Continuous glass fiber length



(a)



(b)

Figure 4.20 Effect of the coupling agent and coir fiber length on flexural properties [(a)Flexural strength, (b)Flexural modulus]

energy absorption per unit volume of the coir fiber did not depend on the length of the coir fiber beyond its critical aspect ratio.

Therefore, the dependence of mechanical properties of the composites on such treatments can be summered as follows:-

1). Increasing the coupling agent concentration would increase is in mechanical properties.

2). An increase of the coir fiber length does not affect the mechanical properties beyond its critical aspect ratio.

4.8.5 The Effect of the Coir Fiber Amount in the Composites

The coir fiber amount in composites greatly affected mechanical properties as shown in Table 4.14. The highest mechanical properties (Tensile properties, compressive properties, and flexural properties except impact strength) fall in the range between 20% to 30% of the coir fiber loading. Figures 4.21 to 4.24 show the effect of the coir fiber loading on tensile properties, compressive properties, flexural properties and impact strength, respectively.

One considers that, below the optimum of fiber content, an increase in fiber content gave the increase in capability of load-bearing of the composites because the fiber remained to serve the ability to bear the load transferred from the matrix; above the optimum fiber content, increase in fiber content gave the decrease in capability of load-bearing of the composites because the fiber could not serve the ability to bear the load transferred from the matrix. The loss of the ability to bear load of the fiber may cause by interfacial voids generated from the difficulty of the matrix to penetrate thoroughly the holes among the fiber. The number of voids along the fiber and matrix would increase according to the amount of fiber loading. In this experiment, the amount of the coir fiber in campsites above 30% would decrease the mechanical properties.

An increase in the amount of fiber would affect two variables of the more ability to bear the load, and the higher number of the voids. These two variables affect the mechanical properties in an opposite direction. Thus an increase in amount of the fiber would give the highest mechanical properties at a specific amount of the fiber. However, the impact strength did not follow the above mentioned statement, an increase in

Table 4.13 Effect of the Coupling Agent on Impact Strength of 20% Coir Fiber-UP Composites at Various Fiber Lengths

Sample	Fiber Length (cm)	Coupling Agent Concentration (%)	Type of Failure	Impact Strength (J/m)
Pure UP Resin	-	-	C*	18.33 ± 4.45
Coir Fiber-UP Resin	1	-	C	82.40 ± 2.92
Coir Fiber-UP Resin	5	-	C	84.50 ± 4.42
Coir Fiber-UP Resin	10	-	C	88.19 ± 6.58
Coir Fiber-UP Resin	Ordinary**	-	C	85.50 ± 3.97
Coir Fiber-UP Resin	1	2	C	117.13 ± 1.37
Coir Fiber-UP Resin	5	2	C	116.57 ± 2.00
Coir Fiber-UP Resin	10	2	C	118.21 ± 1.90
Coir Fiber-UP Resin	Ordinary	2	C	116.33 ± 3.09
Coir Fiber-UP Resin	1	5	C	135.64 ± 3.96
Coir Fiber-UP Resin	5	5	C	144.45 ± 3.76
Coir Fiber-UP Resin	10	5	C	139.94 ± 7.50
Coir Fiber-UP Resin	Ordinary	5	C	142.61 ± 4.66
Coir Fiber-UP Resin	1	8	C	149.60 ± 3.96
Coir Fiber-UP Resin	5	8	C	146.56 ± 4.81
Coir Fiber-UP Resin	10	8	C	144.20 ± 2.28
Coir Fiber-UP Resin	Ordinary	8	C	147.25 ± 3.75
Glass Fiber-UP Resin	1	-	C	413.94 ± 64.34
Glass Fiber-UP Resin	5	-	C	499.47 ± 29.15
Glass Fiber-UP Resin	10	-	C	658.34 ± 70.23
Glass Fiber-UP Resin	Continuous***	-	C	452.77 ± 65.45

* Complete break

** Ordinary length of the coir fiber

*** Continuous glass fiber length

ศูนย์วิทยทรัพยากร
จุฬาลงกรณ์มหาวิทยาลัย

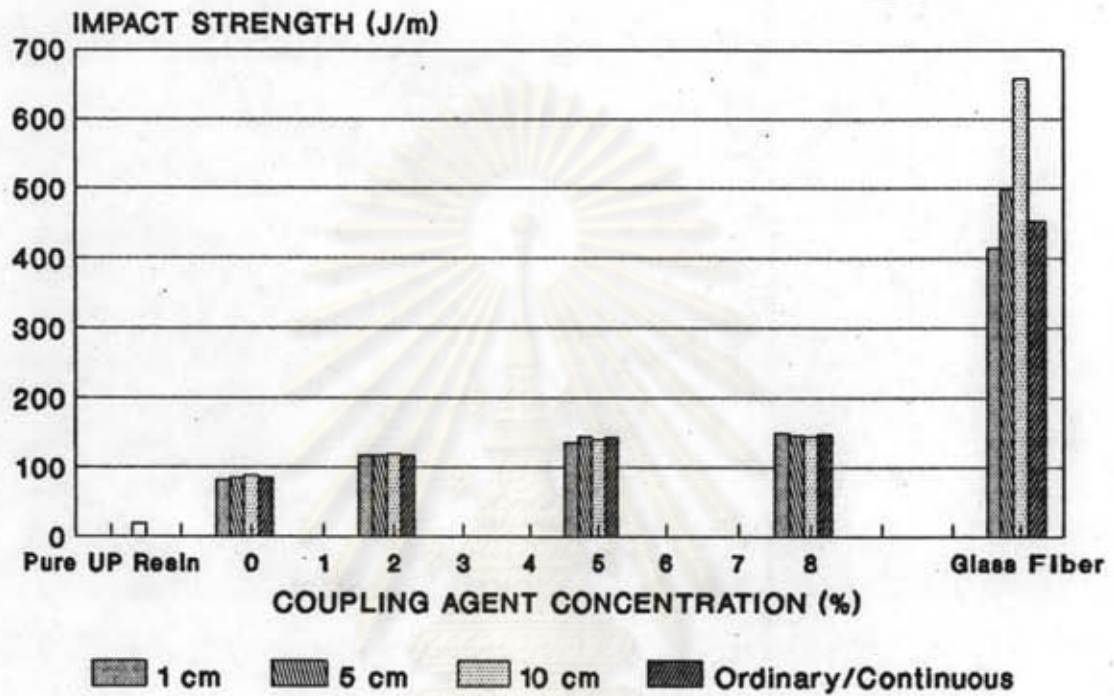


Figure 4.21 Effect of the coupling agent and coir fiber length on impact strength

ศูนย์วิทยทรัพยากร
จุฬาลงกรณ์มหาวิทยาลัย

the fiber amount enhances the degree of the crack stopper which could blunt the crack growth. So the impact strength was increased in a direct proportion to the amount of fiber content according to an increase of the coir fiber amount.



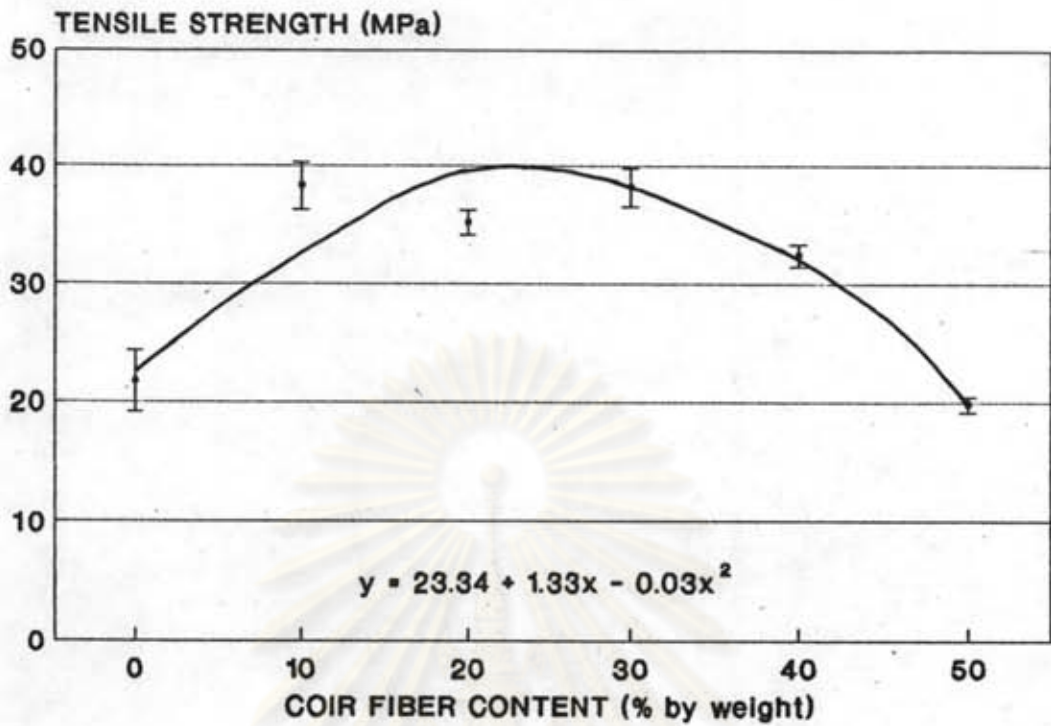
ศูนย์วิทยทรัพยากร
จุฬาลงกรณ์มหาวิทยาลัย

Table 4.14 Effect of the Amount of Coir Fiber in the Composite on Mechanical Properties of the Coir Fiber-UP Composites

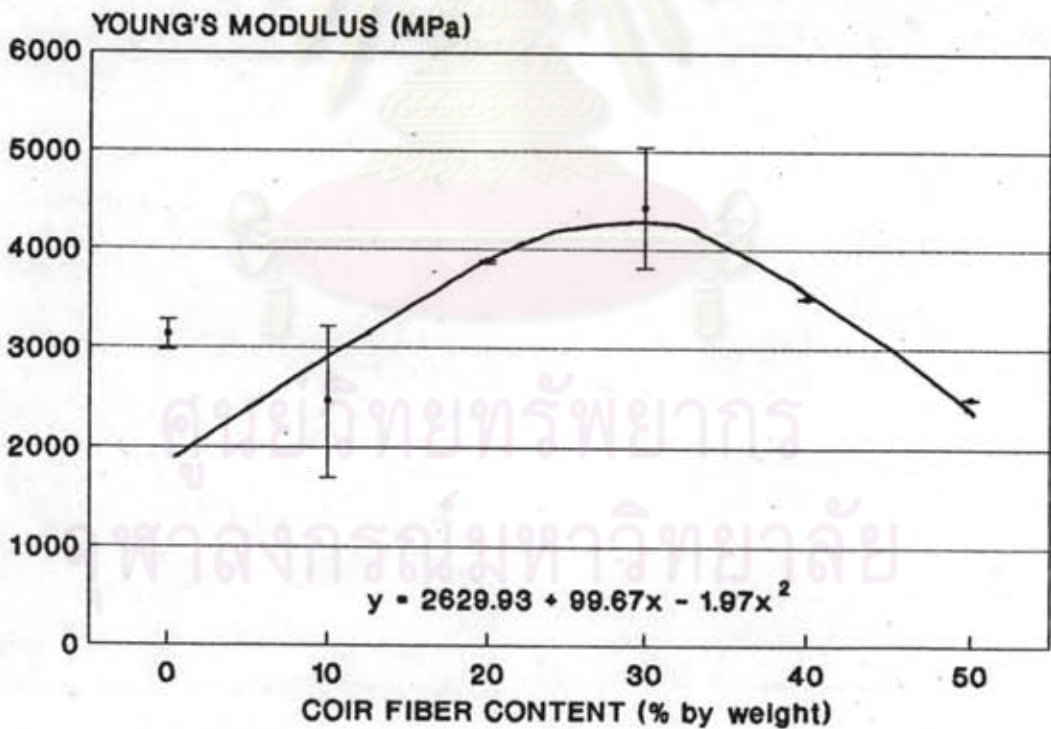
Test Mode	Mechanical Properties	Percent Coir Fiber* in Composites(wt/wt)**									
		10%		20%		30%		40%		50%	
		S.D.***	S.D.***	S.D.***	S.D.***	S.D.***	S.D.***	S.D.***	S.D.***	S.D.***	S.D.***
Tensile Test	Tensile Strength(MPa)	38.31	2.02	35.18	1.08	38.23	1.66	32.40	0.97	19.81	0.66
	Tensile Strain(%)	1.73	0.69	0.94	0.08	0.88	0.06	0.97	0.03	1.17	0.37
	Young Modulus(MPa)	2466	773	3879	13	4428	611	3506	6	2500	10
Compressive Test	Compressive Strength(MPa)	8.472	0.319	10.020	0.210	11.020	1.118	6.929	1.470	7.448	0.372
	Compressive Strain(%)	0.95	0.49	0.64	0.36	0.48	0.31	0.54	0.38	0.97	0.24
	Modulus of Elasticity(MPa)	1777	65	1986	64	2327	7	1489	353	1315	315
Flexural Test	Flexural Strength(MPa)	56.56	1.00	72.04	1.68	76.58	0.84	67.14	1.85	52.77	1.27
	Flexural Strain(mm/mm)	0.0194	0.0040	0.0223	0.0031	0.0260	0.0034	0.0307	0.0049	0.0545	0.0102
	Modulus of Elasticity(MPa)	3187	12	3300	12	3420	9	3196	9	1741	127
Impact Test	Impact Strength(J/m)	123.07	0.98	149.60	3.96	178.03	3.59	190.33	1.35	216.11	4.08

- * Fiber length: 1 cm
- ** Coupling agent: 8%
- *** Standard deviation

ศูนย์วิทยทรัพยากร
จุฬาลงกรณ์มหาวิทยาลัย



(a)



(b)

Figure 4.22 Effect of the coir fiber amount on tensile properties [(a)Tensile strength, (b)Young's modulus]

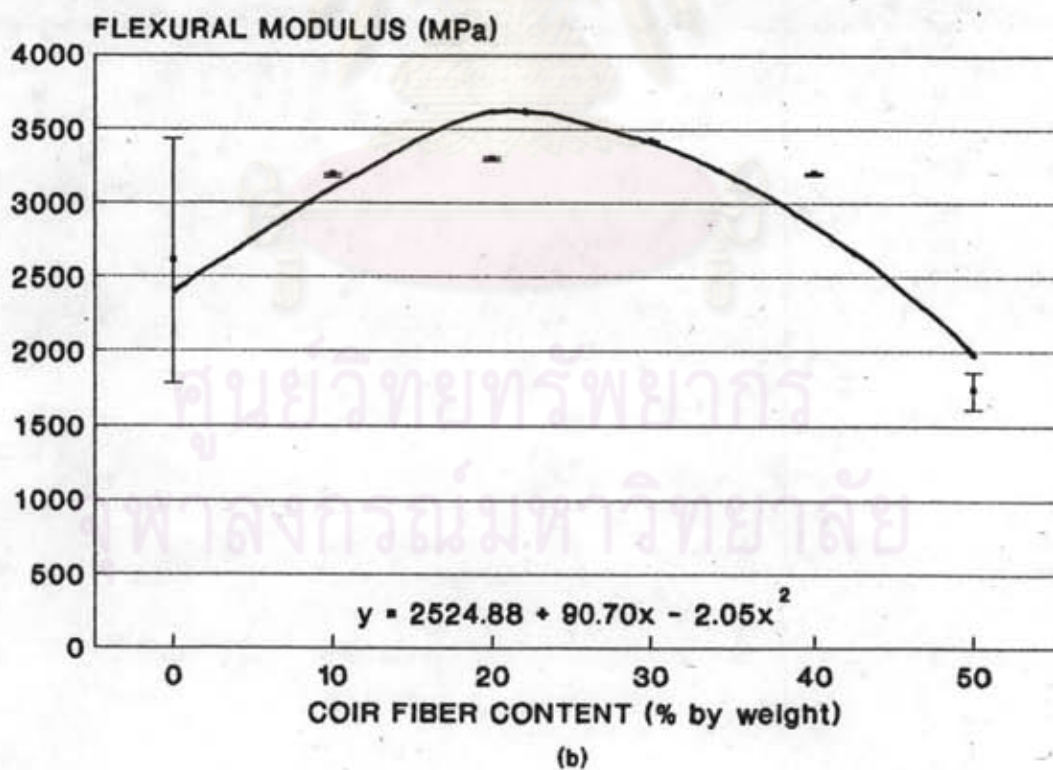
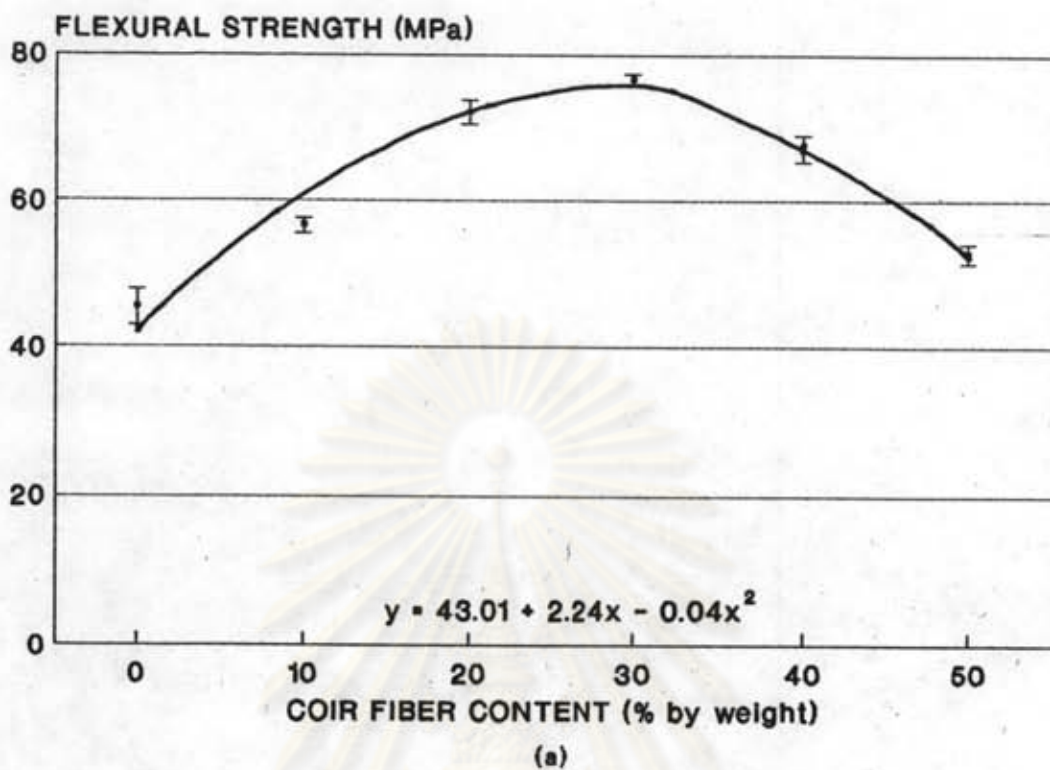
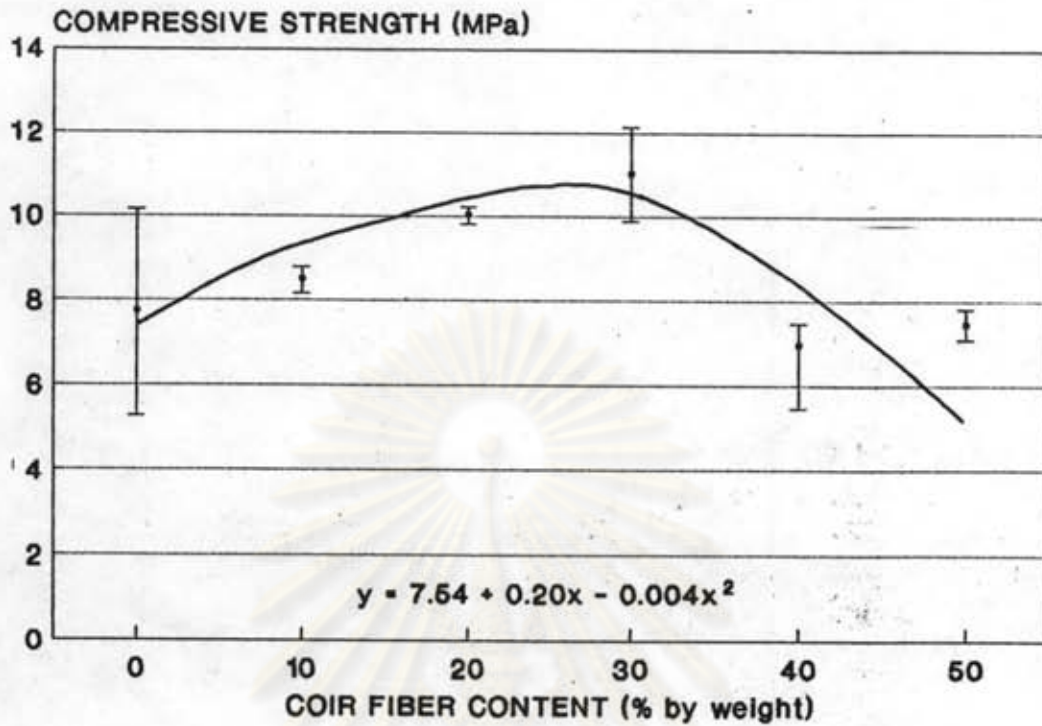
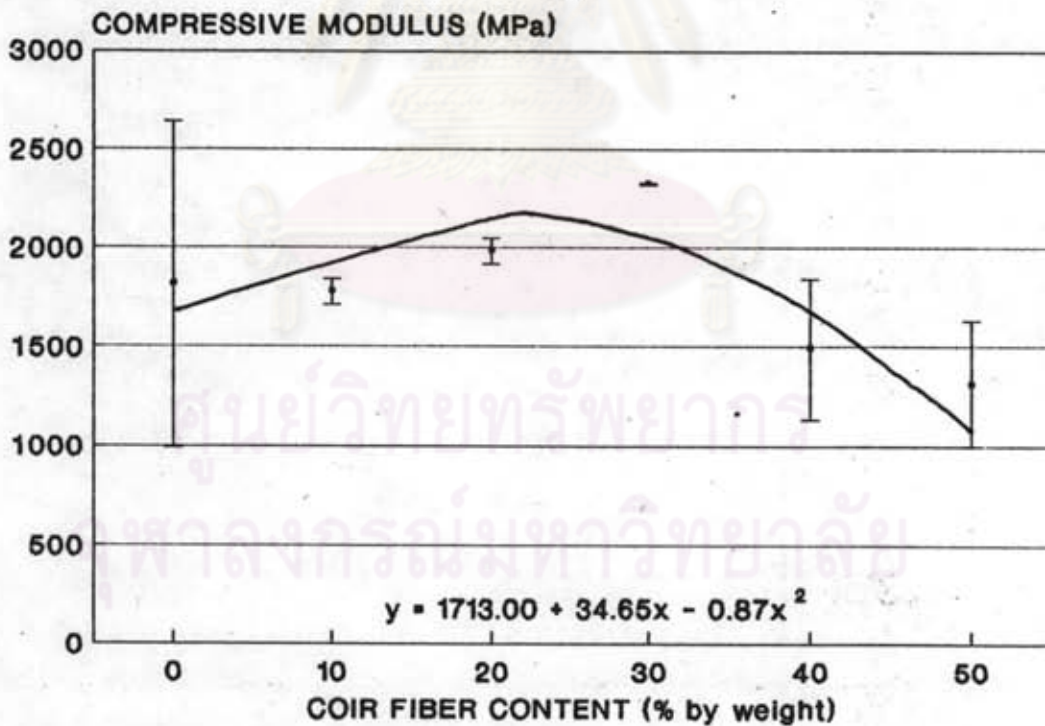


Figure 4.24 Effect of the coir fiber amount on flexural properties
 [(a)Flexural strength, (b)Flexural modulus]



(a)



(b)

Figure 4.23 | Effect of the coir fiber amount on compressive properties [(a)Compressive strength, (b)Compressive modulus]

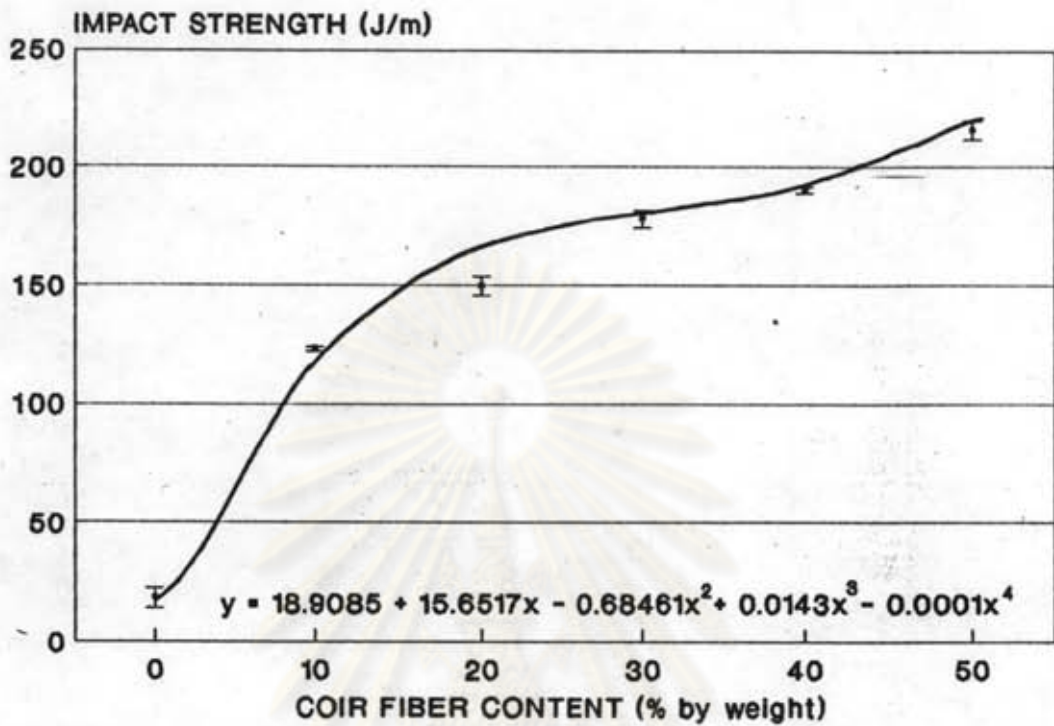


Figure 4.25 | Effect of the coir fiber amount on impact strength

ศูนย์วิทยทรัพยากร
จุฬาลงกรณ์มหาวิทยาลัย